Tephra deposits associated with silicic domes and lava flows

Grant Heiken
Kenneth Wohletz
Earth and Space Sciences Division
Los Alamos National Laboratory
Los Alamos, New Mexico 87545

ABSTRACT

Most phases of silicic lava dome growth have some associated explosive activity. Tephra produced during this activity have depositional characteristics, grain sizes, and grain shapes that reflect different mechanisms of dome growth and destruction. It is therefore possible to interpret the explosive history of a dome through study of adjacent tephra deposits even though the dome may no longer be present.

Five stages of dome growth and their associated tephra deposits are considered here. (1) Crater formation before extrusion of a dome, including phreatic, phreatomagmatic (ph-m), and Plinian pumice eruptions, produces a tephra sequence at the base of a dome consisting of deposits rich in accidental lithic clasts from crater walls, overlain by beds of fine-grained tephra and coarse-grained pumice. (2) Magma pulses during dome growth (ph-m, in part) produce tephra consisting of mixtures of juvenile pumice and clasts derived from the partly solidified dome. (3) Ph-m interaction between new magma and a water-saturated dome produces uniform tephra consisting of angular clasts of dome lava. (4) Explosive eruptions that follow collapse of a gravitationally unstable dome produce tephra that consists of angular, partly pumiceous clasts of dome lava which fragment due to expansion of metastable water after release of confining pressure. (5) Posteruptive destruction of the dome by phreatic eruptions results in pyroclasts consisting of fine-grained, hydrothermally altered clasts derived from dome lavas.

Major kinetic processes before explosive dome eruptions are the relatively slow diffusion of magmatic volatiles from magma to fracture planes and foliations within the dome, and the relatively fast diffusion of meteoric water into magma by mechanical mixing. These basic processes control most explosive activity at domes in cases of either expulsion of new magma or collapse of an unstable dome.

INTRODUCTION

Most phases of silicic dome growth have some associated explosive activity. Tephra produced during these explosive events have depositional characteristics, grain-size distributions, and particle shapes that reflect mechanisms of dome growth and destruction. Hopson and Melson (1984) have interpreted Mount St. Helens' pre-1980 history (both constructional and destructional) from a study of older dome remnants and pyroclastic deposits exposed in and around the crater formed in 1980. Explosive activity associated with volcanic dome growth has been analyzed in detail by Newhall and Melson (1983) with regard to history, rate of growth, and petrologic controls of explosions. They point

out the "conventional wisdom" that dome growth is a late-stage phase that follows explosive activity. Their analysis of historic eruptions indicates that explosive activity is, however, associated with all stages of dome growth.

Water plays an important role in all explosive activity associated with dome growth and destruction. Dome emplacement is commonly preceded by explosive Plinian and phreatomagmatic (ph-m) eruptions, each with both magmatic and meteoric water as a main volatile component and driving medium. Water is also important in the formation of steam within domes that are destroyed, in part by collapse and subsequent explosions, or by

TUFF RING AND TUFF CONE
WITH OVERFLOWING LAVA PLUG

COALESCING DOMES WITH PHREATIC
AND PHREATOMAGMATIC CARAPACES

EXPLOSION CRATER

PLINIAN, FAR-FIELD, PUMICE FALLS AND
FLOWS, PELÉEAN AVALANCHE DEPOSITS

POLYGENETIC DOME GROWTH
WITH INTERCALATED FLANK DEPOSITS
(COMPOSITE CONE)

STRATIGRAPHIC ASSOCIATIONS – DOMES AND TEPHRA DEPOSITS
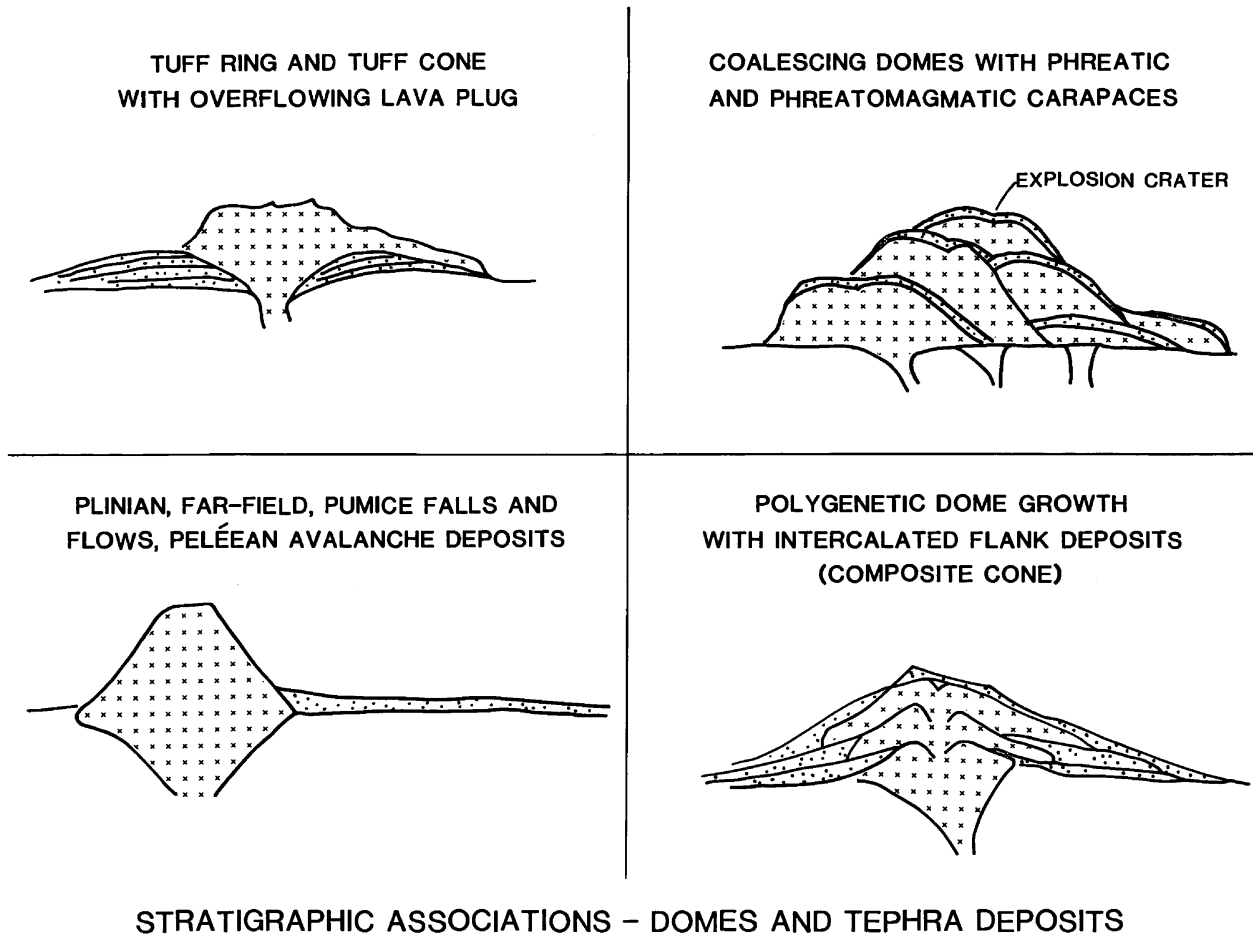
Figure 1. Schematic cross sections illustrating common occurrences of dome-related tephra deposits.

phreatic, crater-forming blasts. Water is also involved in the hydrothermal alteration of dome lavas and in their gravitational collapse because of structural weakening.

On the basis of a review of a number of dome-related tephra deposits, we propose the following eruptive types to classify tephra of similar characteristics: (1) Plinian and phreatomagmatic tephra eruptions preceding dome emplacement; (2) Vulcanian tephra related to periodic and continuing dome growth; (3) Peleean and Merapian tephra associated with dome destruction; and (4) phreatic tephra (from explosively active hydrothermal systems). The tephra of these eruption types occur in a variety of geologic situations (Fig. 1).

We describe tephra by several characteristics, including deposit volume and emplacement mode, tephra-size distributions, constituents, chemical composition, and grain textures as determined by scanning electron microscopy (SEM). The SEM studies are emphasized because they present the most distinguishing data for tephra characterization.

PLINIAN PUMICE AND PHREATOMAGMATIC DEPOSITS THAT PRECEDE DOME EMPLACEMENT

Most silicic domes are extruded at the end of an eruption cycle that begins with highly energetic, gas-rich eruptions that produce Plinian pumice deposits and associated pyroclastic flows. If there is ample ground or surface water close to the vent, phreatomagmatic activity can produce fine-grained silicic tephra that are present both as a widespread deposit and proximal tuff ring through which the dome is later extruded (Fig. 2). Several examples are used here, including Plinian pumice deposits in the Medicine Lake Highland, Chaos Crags, and Panum Crater, California. These deposits have small volumes (<0.5 km^3), are associated with fissure eruptions of silicic magma, and are overlain by silicic domes.

Little Glass Mountain and Glass Mountain

Models for dome formation and growth were developed by

INITIAL PLINIAN AND PHREATOMAGMATIC ERUPTION
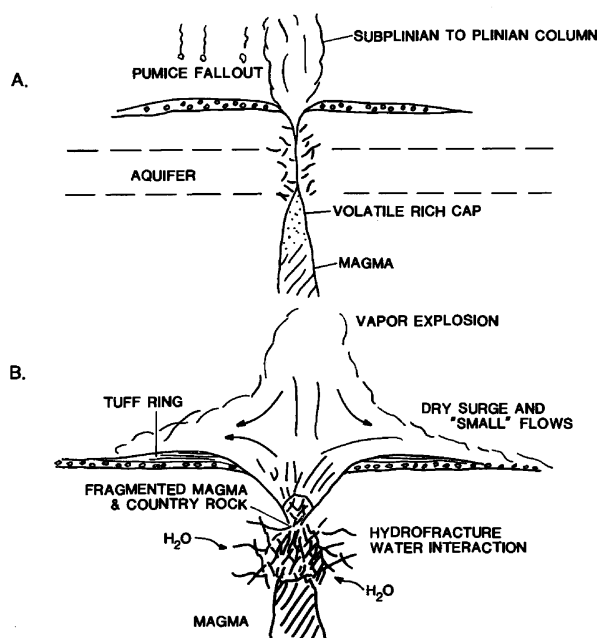
Figure 2. Schematic illustration of tephra production preceding dome formation with a Plinian stage (A) followed by phreatomagmatic explosions (B).

TABLE 1. SUMMARY OF HOLOCENE SILICIC ERUPTIONS, CHAOS CRAGS AND MEDICINE LAKE HIGHLAND, CALIFORNIA*

	Chaos Crags	Medicine Lake Highland
Total volume	1.4 km³	1.2km³
Tephra volume	10% of total	10% of total
Main mode of tephra deposition	pyroclastic flow	Plinian ash flow
Phenocryst content of pumice	30-40%	0-trace
Pumice characteristics: Vesicularity	14-30%	50-60%
Predominant vesicle shape	ovoid; little coalescence	highly elongate; coalesced vesicles
Glass composition	rhyolite	rhyolite
Mixed magma	>90%	10%

*From Heiken and Eichelberger (1980).

Fink (1983) at the Little Glass Mountain and Glass Mountain, California, rhyolite flows. Emplacement of each dome complex was preceded by a Plinian eruption. Pumice-fall deposits from these eruptions range in thickness from 4 to 6 m near the vent, to a few cm at a distance of 25 km from the source (Table 1). There are only small pumice rings developed around vents. Most of the pumice beds consist of multiple, 20- to 50-cm-thick, reversely graded beds of pale-gray pumice lapilli and coarse ash (Heiken, 1978). Pumice beds drape underlying terrain and exhibit no flowage structures. All tephra units consist of very poorly sorted lapilli and are within the grain-size field of tephra-fall deposits as described by Walker (1971).

Pumice pyroclasts (Fig. 3A) are equant to slightly elongate and have sharp, angular surfaces. Most have 40% to 50% vesicles; vesicles are 10 to 500 μm long and are highly elongate. Pumices from both vents (Glass Mountain and Little Glass Mountain) are remarkably homogeneous throughout the eruption sequence. Blocky grain surfaces are both parallel and normal to the long axes of vesicles. Most pumices contain some cavities that consist of partly collapsed vesicles surrounded by elongate vesicles. All pumices consist of aphyric glass; only samples from Little Glass Mountain contain traces of orthopyroxene phenocrysts.

Pumice pyroclasts in these deposits are highly vesicular and lack phenocrysts, indicating rapid rise of magma along dikes. All pumiceous pyroclasts have parallel vesicles with high aspect ra-

tios. Vesicles appear to have formed prior to eruption and were stretched during flow, parallel to dike walls. Angular fractures are oriented parallel and normal to elongate vesicles and form a distinctive type of pyroclast; these may have formed by disruption of vesiculating magma by passage of a rarefaction wave downvent. Fragmented, vesicular clasts were then accelerated out of the vent (an idea that was first proposed by Rittman, 1936). After the volatile-rich top of the magma body was erupted as tephra, the bulk of dome lavas with low (<20%) vesicularities were erupted (Fink, 1983). A total volume of 1.2 km³ was erupted during this Holocene rhyolitic event; 10% of that volume (dense-rock equivalent) consists of pumice deposits erupted before the domes (Heiken, 1978).

Chaos Crags, California

The Chaos Crags are a line of Holocene age dacite domes located immediately north of Lassen Peak, California. Prior to eruption of these domes, explosive activity produced ash falls and pyroclastic flows of small volume (Table 1). The pyroclastic-flow deposits consist of massive, nonwelded coarse ash that, in some places, contain large pumice lapilli and blocks. Beds with more than 10% blocks and bombs are reversely graded. Ash-fall beds consist of massive and normally graded medium to fine ash and lapilli-bearing coarse ash (Heiken and Eichelberger, 1980).

In contrast to the aphyric, highly vesicular pumice pyroclasts of Glass Mountain and Little Glass Mountain, Chaos Crags pumices are porphyritic and poorly vesicular. Vesicularities range from 6% to 46%, but the average is about 30%. Vesicle shapes range from spherical to highly elongate, but most are ovoids, 10–200 μm long. Pumices contain between 30% and 45% anhedral to subhedral phenocrysts of plagioclase, hornblende, biotite, quartz, and magnetite. Many vesicles in these pyroclasts radiate from phenocryst surfaces.
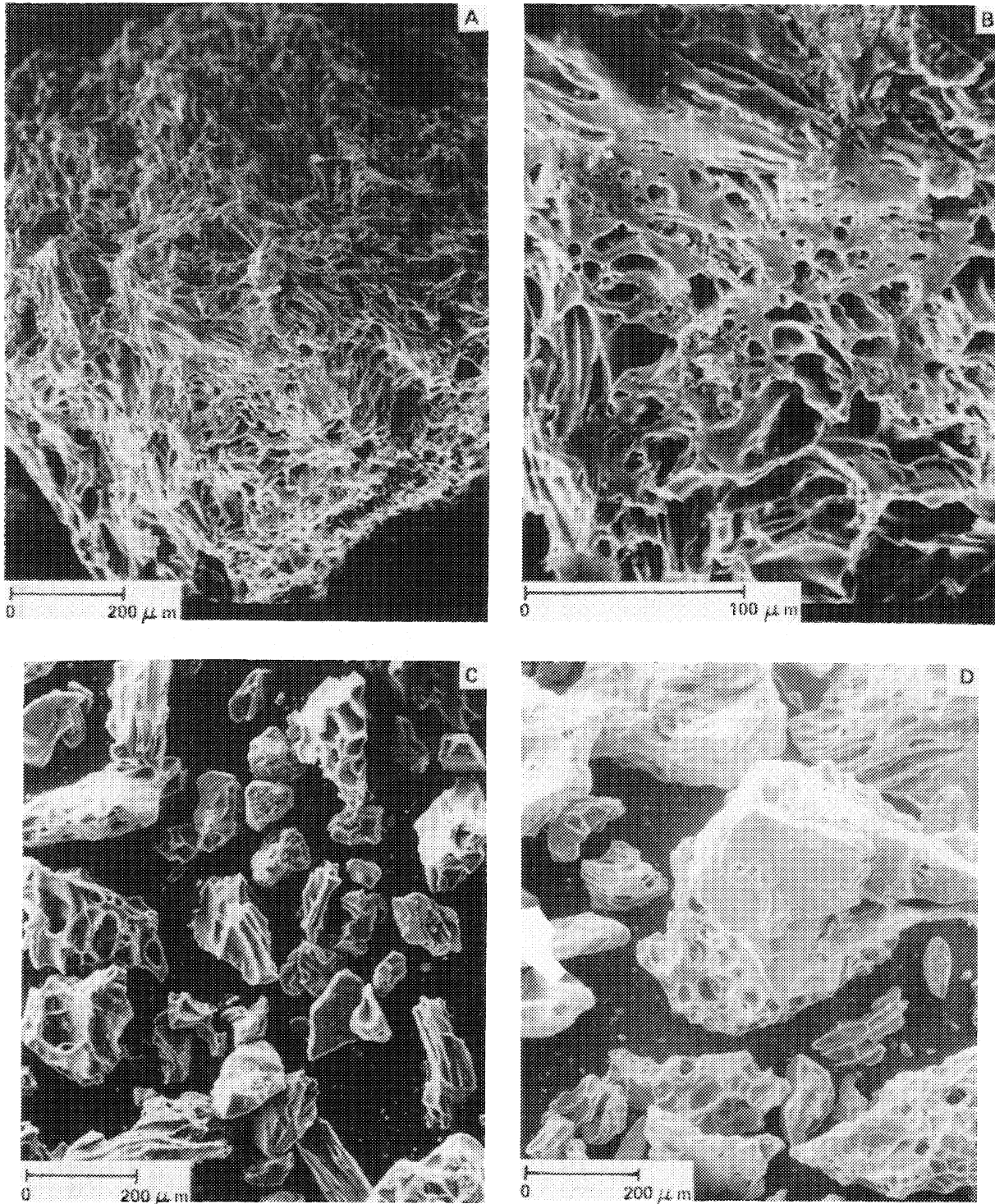
Figure 3. Scanning electron micrographs of pumice pyroclasts from Glass Mountain, Medicine Lake Highland, and Chaos Crags, California. *Glass Mountain.* A: Angular, subequant rhyolitic pumice. It is all glass and contains no phenocrysts. This is an "end-on" view of the pyroclast; short axes of highly elongate vesicles are shown. Larger cavities are composite and were formed by coalescence of adjacent vesicles. B: Detail of A showing the variation in vesicle widths. Most vesicles are thin walled, and many exhibit some degree of coalescence. *Chaos Crags.* C: This tephra consists of a mixture of pumice and crystal pyroclasts. Pumices are ash size and angular, and contain mostly thick-walled, ovoid vesicles. D: Another tephra pumice and phenocrysts are coated with pumiceous glass.

PANUM CRATER

Column	Sample	Description
	5	Planar $Md_\phi = -0.18, \sigma_\phi = 2.06$
	4	Coarse Sandwave $Md_\phi = 0.29, \sigma_\phi = 1.18$
		Sandwave
	3	Sub-plinian fall $Md_\phi = 0.66, \sigma_\phi = 2.53$
	2	Sandwave $Md_\phi = 2.83, \sigma_\phi = 0.98$
		Massive Planar
	1	Explosion breccia $Md_\phi = 1.80, \sigma_\phi = 2.09$
		Flow breccia

2m

0
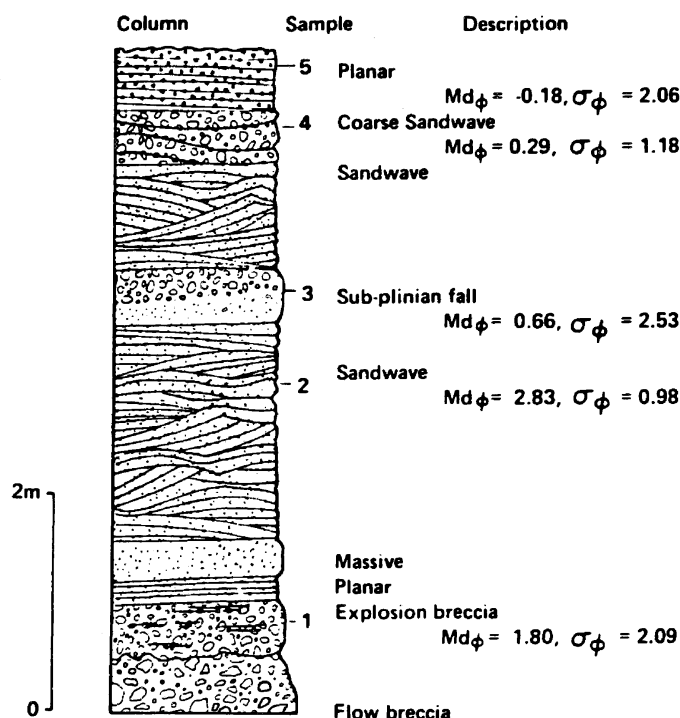
Figure 4. A stratigraphic section of the basal part of the Panum Crater tuff ring showing the sequence of mainly pyroclastic surge deposits with one subplinian pumice bed. The upper portion of the section (not illustrated) consists of repetitions of planar bedding shown at sample interval 5. Note the tephra size parameters for each studied sample.

TABLE 2. CHEMICAL ANALYSES OF PANUM CRATER PYROCLAST SURFACES IN WT%[*]

	1	2	3	4	5
SiO_2	67.72	72.45	69.90	68.45	70.83
TiO_2	2.14	1.64	2.02	2.22	1.79
Al_2O_3	13.49	12.62	12.92	12.86	13.02
FeO	3.692	1.97	2.64	3.13	1.29
MnO	1.86	1.26	1.62	1.98	1.40
MgO	1.59	1.30	1.54	1.51	1.48
CaO	2.40	1.85	2.23	2.34	2.01
Na_2O	1.37	1.39	1.67	1.50	1.52
K_2O	5.80	5.55	5.94	6.01	5.77
Glass	85.9	74.0	83.0	87.0	83.0
Crystal	4.7	24.0	12.5	8.0	12.0
Lithic	9.4	2.0	4.5	4.8	4.0

[*]Normalized standardless energy dispersive spectral analyses of grain surfaces.

Pumice from the Chaos Crags eruption have low vesicularities; lower volatile contents may have been related to crystallization of a hydrous phase (Fig. 3b). Vesiculation appears to have occurred near surface where there was little chance of vesicle elongation by flow. As in the Medicine Lake Highland, tephra from Chaos Crags make up about 10% of the total volume erupted (dense-rock equivalent; DRE); 1.1 km^3 is lava erupted as a stubby flow and a three-lobed dome.

Panum Crater, California

Panum Crater is a Holocene-age rhyolite dome surrounded by a tuff ring 600–700 m in diameter. It erupted at the northern end of the Mono Crater chain in east-central California (Putnam, 1938; Kistler, 1966; Sieh, 1983). Its opening explosive eruptions have been dated by Wood (1977) at 1190 ±80 yr B.P.

To illustrate the sequence of pyroclastic material constituting the tuff ring we include here a stratigraphic section measured in a pumice quarry on the ring's southeast flank (Fig. 4). The initial explosive eruptions produced an explosion breccia, which is overlain by dominantly dune-bedded pyroclastic surge beds

with an intercalated sub-Plinian pumice- and ash-fall layer. The last explosive activity, prior to dome extrusion, deposited planar-bedded surge deposits that formed upper portions of the ring. The volume of these tephra is estimated to be between 0.005 and 0.05 km^3.

Pyroclast size data, shown in Figure 4, display a gradual coarsening of tephra upward in the section from a median diameter of about 150 μm to 1 mm. The dune-bedded materials are well sorted, whereas the fall and planar-bedded surge deposits are moderately to poorly sorted.

Phenocryst-poor rhyolite magma was erupted at Panum Crater. Grain surface alteration is slight on all samples except those of the lower strata, where coatings and vesicle fillings of altered glass and claylike material are visible. Chemical changes on tephra surfaces, caused by rapid posteruptive surface alteration, is typical of phreatomagmatic eruptions (Table 2) (Heiken and Wohletz, 1985). Accidental lithic pyroclasts constitute nearly 10% of early explosion materials and about 5% of later tephra. Variation of phenocryst abundance throughout the eruption sequence is also evident (Table 2). This variation and the degree of glass alteration (i.e., deviation from expected rhyolite compositions), explain differences in chemical compositions throughout the eruption sequence.

Surface textures (Fig. 5) of vitric pyroclasts are dominated by blocky and equant shapes and minor to moderate development of vesicles (Table 3). Where present, vesicles are cut by planar to curviplanar fracture surfaces; fine dust particles adhere preferentially to vesicle surfaces. Many vesicles, especially those of later erupted tephra, are elongate and range from parallel tubelike hollows to flattened ellipsoids that define a foliation that is also apparent in later extruded lavas. Overall, vesicle abundance appears to decrease upward in the section. Abrasion features on grain surfaces are poorly to moderately developed and consist of some rounding of initially sharp edges, chips, grooves, and conchoidal-like fracture planes.
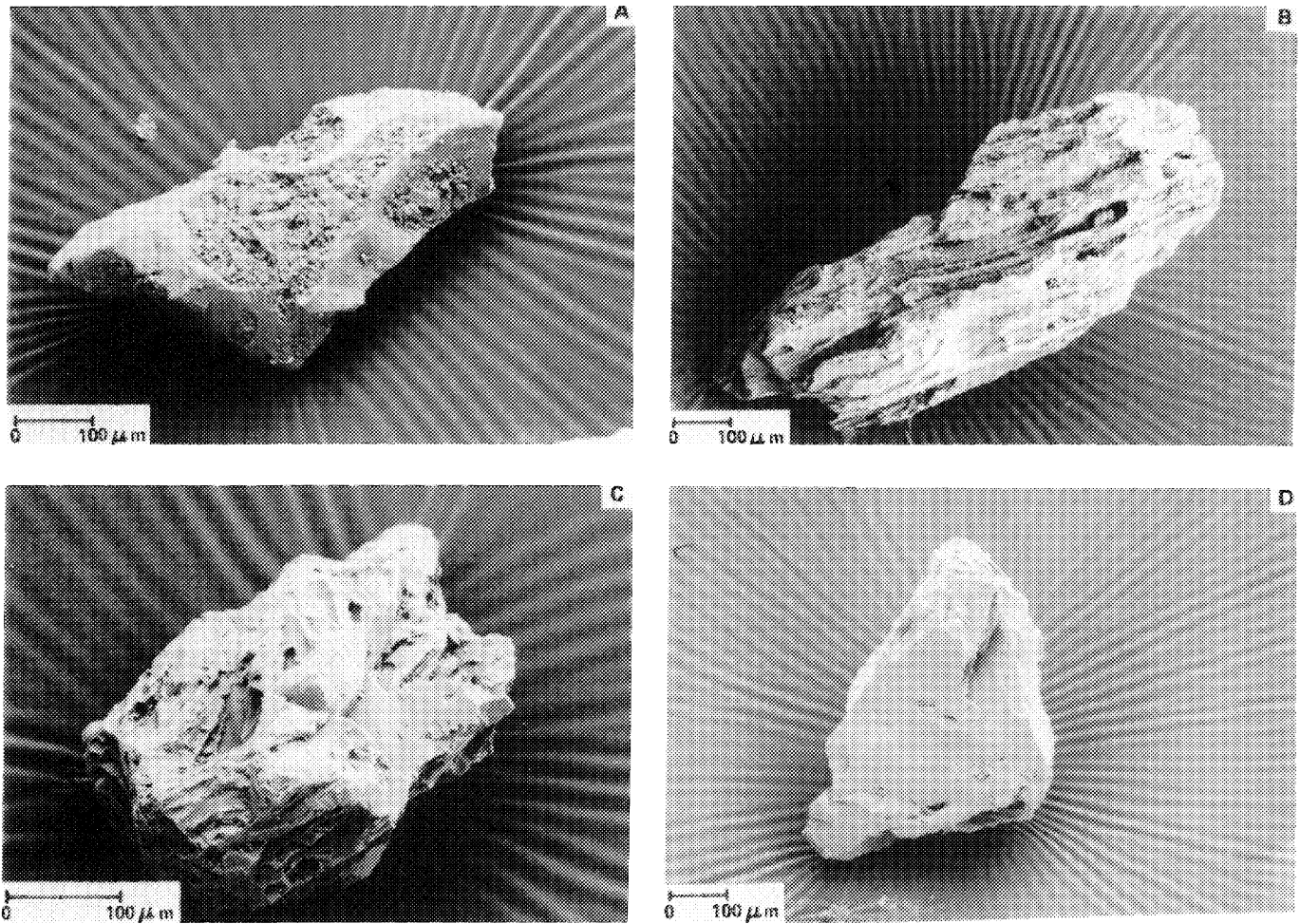
Figure 5. Stratigraphic column (top) and scanning electron micrographs (SEM) (bottom) of Panum Crater tephra. SEM show typical features of silicic, dominantly phreatomagmatic ash. A: Poorly vesicular slablike grain from the explosion breccia, sample 1. Vesicle is filled with fine ash and some alteration products, and the grain surface is coated with hydrated glass. B: Blocky, vesicular grain from sandwave sequence, sample 2. This grain has several planar fracture surfaces and edges are partly rounded by transport abrasion. C: Pumiceous equant grain from Subplinian bed, sample 3. Although vesicular and displaying several surfaces bounded by curved vesicle walls, this grain is also somewhat blocky, which probably indicates fragmentation in part by quench stresses during phreatoplinian eruption. This sample best matches Wood's (1977) tephra #2 that is widely distributed over the southeastern Sierra Nevada. D: Angular, blocky ash grain from the upper portion of the measured section, sample 5; the poor vesicularity, rounded corners, and surface pits, chips, and scratches typify ash formed by late-stage phreatomagmatic fragmentation of the viscous, volatile-poor magma erupted just prior to passive lava dome extrusion.

Tephra produced by the opening eruptions are dominantly phreatomagmatic and subordinantly magmatic phreato-Plinian, because vesiculating rhyolite magma was extruded through water-saturated alluvial deposits present around Mono Lake.

VULCANIAN ERUPTIONS ASSOCIATED WITH DOME GROWTH

Vulcanian activity encompasses a wide range of eruption phenomena; this range includes tephra emission during formation of silicic domes and plugs at polygenetic volcanoes (Fisher and Schmincke, 1984). These volcanoes may be dome complexes or composite cones that display periodic and, in some cases, cyclic tephra emissions. This activity has its name derived from the Aeolian island Vulcano, in the Tyrrhenian Sea, where Mercalli and Silvestri (1891) witnessed and described the 1888–1890 eruption of the Fossa cone. In that eruption, intermittent, staccato, and cannon-like bursts of ash and accretionary lapilli

TABLE 3. TEXTURAL FEATURES OF PANUM CRATER TEPHRA PARTICLES

Sample and Bed Form*	Grain Shape	Edge Modification	Alteration	Fine Fraction (wt.%)	Distinguishing Features
1 M	vesicular, blocky	subangular smooth rounded vesicle edges	moderate with vesicle fillings	blocks and plates, some adhering dust (9%)	vesicular with lithic material
2 SW	blocky	subangular, grooves, dish shape fractures	slight, mostly clean surfaces	very thin plates, abundant micrometer-size dust (11%)	impact fractures
3 F	blocky, vesicular	angular, none	slight, clean surfaces	blocks and plates, no fine dust (5%)	no abrasion
4 SW	blocky, vesicular	subrounded, stepped and dish shape fractures	slight, vesicle fillings	blocks, adhering dust (1%)	highly abraded edges
5 P	blocky	angular, chipped edges	none	blocks, no adhering dust (2%)	clean surfaces, few vesicles

*Bed forms are: SW - sandwave, M - massive, P - planar, F - fall.

that produced bedded ash falls, surges, and lahars on the slopes of the Fossa cone were followed by quiet periods of several minutes to several days. Early eruptions ejected dominantly accidental lithic ash derived from old vent lavas. Later explosions produced juvenile blocks, breadcrust bombs, and ash.

Much Vulcanian activity can be attributed to ground water in contact with new magma below the cone, whereas later explosions are caused by vesiculating magma (Fig. 6). The three examples described below include tephra associated with renewed activity at Vulcano in 1888 and continuing dome growth at Mount St. Helens, Washington, and Santiaguito, Guatemala in recent years.

Vulcano, Italy; 1888–1890 Eruption

Recent studies by Sheridan and others (1981) and Frazzetta and others (1983) carefully documented pyroclastic materials deposited during the Vulcanian eruptions of 1888–1890. By comparing these deposits with those of earlier eruptions, these workers illustrated the clear recurrence of Vulcanian activity. Figure 7 is a stratigraphic section of the four most recent eruption cycles and shows a progression for each cycle, from explosion breccia (partly destroying the previous plug) to ash fall to wet and dry surge eruptions; these are followed by pumice falls and lava-flow extrusion. Much of the tephra deposited on volcano slopes was remobilized as lahars and moved off cone slopes.

Typical tephra deposits consist of ash and lapilli falls, sets of thinly bedded coarse and fine ash, dry surge dunes and planar beds, and wet-surge beds that are transitional to lahars. The total volume of tephra from the 1888–1890 eruption cycle is estimated to be in the range of 0.01 km³. Most samples are characterized by two size populations with dominant modes at 0.5 to 1.5 ϕ and
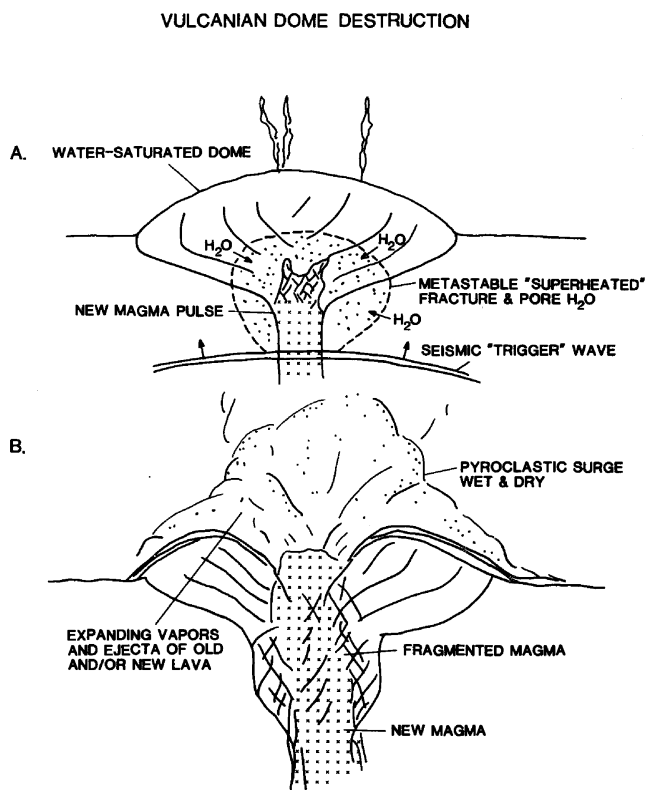
Figure 6. Schematic illustration of preeruptive (A) and eruptive (B) stages for an example of Vulcanian activity.
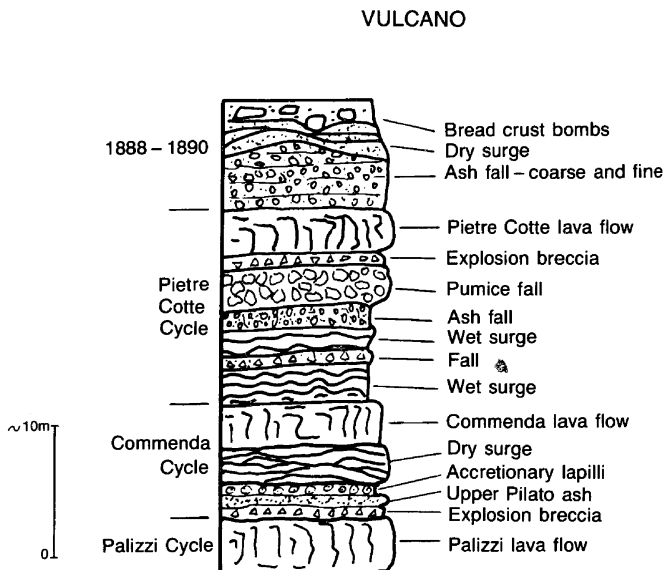
VULCANO

Figure 7. Stratigraphic columnar section adapted from Frazzetta and others (1983) of the past four eruptive cycles at Vulcano. The most recent cycle, 1888–1890, typifies Vulcanian activity associated with silicic lava extrusion; samples from this deposit are described.

2.5 ϕ to 3.5 ϕ; however, ash and lapilli falls commonly show an additional mode in the range of –2.0 ϕ to –1.0 ϕ. Wet-surge deposits are typically very fine grained and have a mode finer than 4.5 ϕ. The significance of tephra size modes has recently been discussed by Frazzetta and others (1983, 1984), who ascribed them to traction, saltation, and suspension modes of transport.

On the basis of tephra petrography, Frazzetta and others (1983) suggested that mixing of evolved aphyric rhyolite and tephrite magmas occurred at Vulcano. A variety of phenocrysts are noted in the tephra. Phenocrysts of clinopyroxene, calcic plagioclase, and olivine are entirely free of glass coatings and have cleavage faces modified by stepped fractures and some shallow, dish-shaped concavities (Fig. 8A). Glass particles are poorly vesicular to nonvesicular (Fig. 8B) and have blocky shapes with sharp, acute edges and broad curviplanar surfaces. Abrasion has rounded some grain surfaces; these surfaces were also pitted and coated during postdepositional solution and precipitation. Rare pyroclasts with fluidal and ropy surfaces formed from fragmented portions of the mafic-melt fraction.

Many of the glassy tephra are accidental lithic clasts derived from older dome lavas. This is characteristic of Vulcanian tephras, which generally display marked surface hydrothermal alteration that produces a coated or "muddy" surface texture.

Mount St. Helens; Continuing Dome Growth

Considerable scientific attention on the continuing activity at Mount St. Helens since 1980 has greatly increased our aware-

ness of the complexities of dome growth (see Swanson and others, this volume; Hopson and Melson, 1984). This activity has taken place over 6 years as intermittent eruptions of dacite lava flow lobes of small volumes (1–4 × 10^6 m^3); tephra emissions associated with some of these magma pulses produced plumes several thousand metres high and small pyroclastic flows and lahars (Swanson and others, 1983; Waitt and others, 1983). Tephra volumes are much less than those of the associated lavas. These authors have noted some correlation of the amount of snowpack present and the magnitudes of small explosions.

The tephra samples discussed here were provided by Don Swanson, who collected them in April 1983 from snow on the crater floor about 400 m from the vent. Tephra characteristics discussed here are solely those obtained from SEM observation. Coarser materials were carbon coated for low resolution (50 to 1000 X) imaging and semiquantitative energy dispersive spectral (EDS) analysis. Fine fractions were gold coated for high resolution (3 000 to 30,000 X) imaging.

The samples are fine- to medium-ash size; the largest clasts are in the range of 500 to 900 μm and there is abundant material in the size range of 50 to 125 μm; the finest material is 0.2- to 1.0-μm-size dust attached to 1 to 15 μm particles.

Textural features (Fig. 9) of the ash are presented in Figure 10 as percentage abundance of a textural feature in each sample (from grain counts of scanning electron micrographs). These data are plotted as a function of stratigraphic position and reveal tephra properties related to eruptive mechanism as discussed by Wohletz and Krinsley (1982). Several features are readily apparent and can help in understanding tephra production related to dome growth (Fig. 10): (1) vesicularity is generally low (<10%) for coarse particles but higher (10–70%) for fine ones; (2) blocky, equant grain shapes have an inverse relationship to vesicularity (pyroclast textures are dominantly blocky); (3) fused and fluidal grain surfaces are more apparent in the fine fraction than in the coarse fraction, but the opposite relationship is noted for grain-surface alteration. Fused surfaces indicate something about the viscosity, and hence, the temperature of the fragmented lava; (4) fine adhering dust is noted on about 40% of all particles and is most prevalent on fine-grained particles. The finest ash is most abundant in eruptions of the most fluidal and hottest magmas, and (5) the abrasion of coarse particles is low (15–30% of the particles) and most likely represents reworking of accessory fragments derived from pulverization of dome lavas and older tephra. Accessory grains generally appear to be the most hydrothermally altered and pose a problem for SEM viewing because their surfaces collect a substantial charge under the electron beam.

Semiquantitative measurement of major-element abundances on grain surfaces is illustrated in Figure 11. The variation of elemental abundances among samples might seem surprising; however, it simply shows that the amount of grain surface alteration is strongly controlled by hydrothermal processes within the dome before and during each ash-eruption pulse. The analyses are compared with average values for the 1980 to 1982 dome
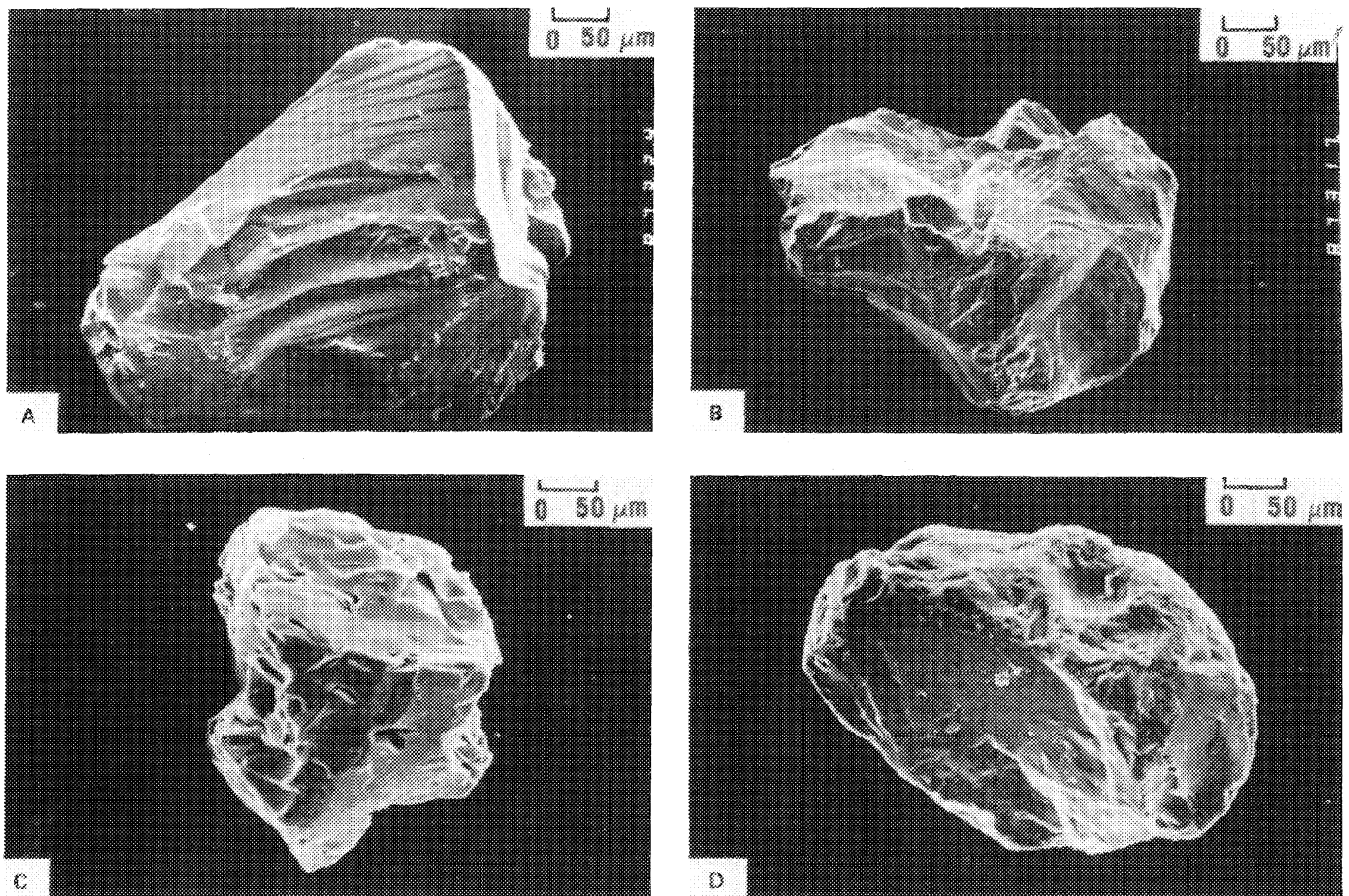
Figure 8. A, B: Scanning electron micrographs (SEM) of crystal pyroclasts from Vulcano. Note cleavage faces modified by stepped fractures. C, D: SEM of glass pyroclasts from Vulcano. These poorly to nonvesicular grains show some abrasion rounding, chipping, and pitting.

lavas and pumice of the AD 1500, 1800, and 1980 eruptions reported by Cashman and Taggart (1983) and Melson (1983). In all cases, the average composition found for all tephra surfaces is very close to that of the dome lavas. It is interesting to note that these analyses vary with samples in a similar fashion as do textural features discussed above. If the limitations of EDS analysis of particle surfaces are considered, it is difficult to know the exact meaning of the values obtained; however, we have noted similar variations of tephra surface chemistry in a number of tephra sequences studied from other volcanoes (Heiken and Wohletz, 1985). A conservative interpretation is that varying eruption processes within the dome are reflected in the degree of hydrothermal alteration of tephra. Analytical values (especially SiO_2) are both the most similar and the most dissimilar to those of pumice from past explosive eruptions for samples that show the greatest phreatomagmatic textural components of blockiness and surface alteration. Vesicularity is greatest for samples most similar to those of dome lavas.

Our interpretation of this complex data set is mostly independent of any field data. We believe that both magmatic and phreatomagmatic mechanisms play a part in eruption of tephra from the dome at Mount St. Helens, and that the relative dominance of these mechanisms alternate sequentially with time. Overall tephra vesicularities are relatively low when compared with tephra of magmatic eruptions. Therefore, phreatomagmatic eruptions most likely produced most of the tephra and may be controlled by the rate of ground-water flow derived from snowmelt and rainfall and the rise rate of new magma. In this situation, phreatomagmatic activity encompasses direct contact of fluid magma with ground water and the development of an unstable hydrothermal system around congealing subsurface magma. Because vesicularity, adhering fine dust, and fused surfaces are most prevalent in the fine-fraction tephra, these particles likely represent the magmatic component of the samples, whereas coarse-fraction materials reflect more of the phreatic accessory and phreatomagmatic constituents.

Santiaguito, Guatemala

Santiaguito is a dome complex in southwest Guatemala that
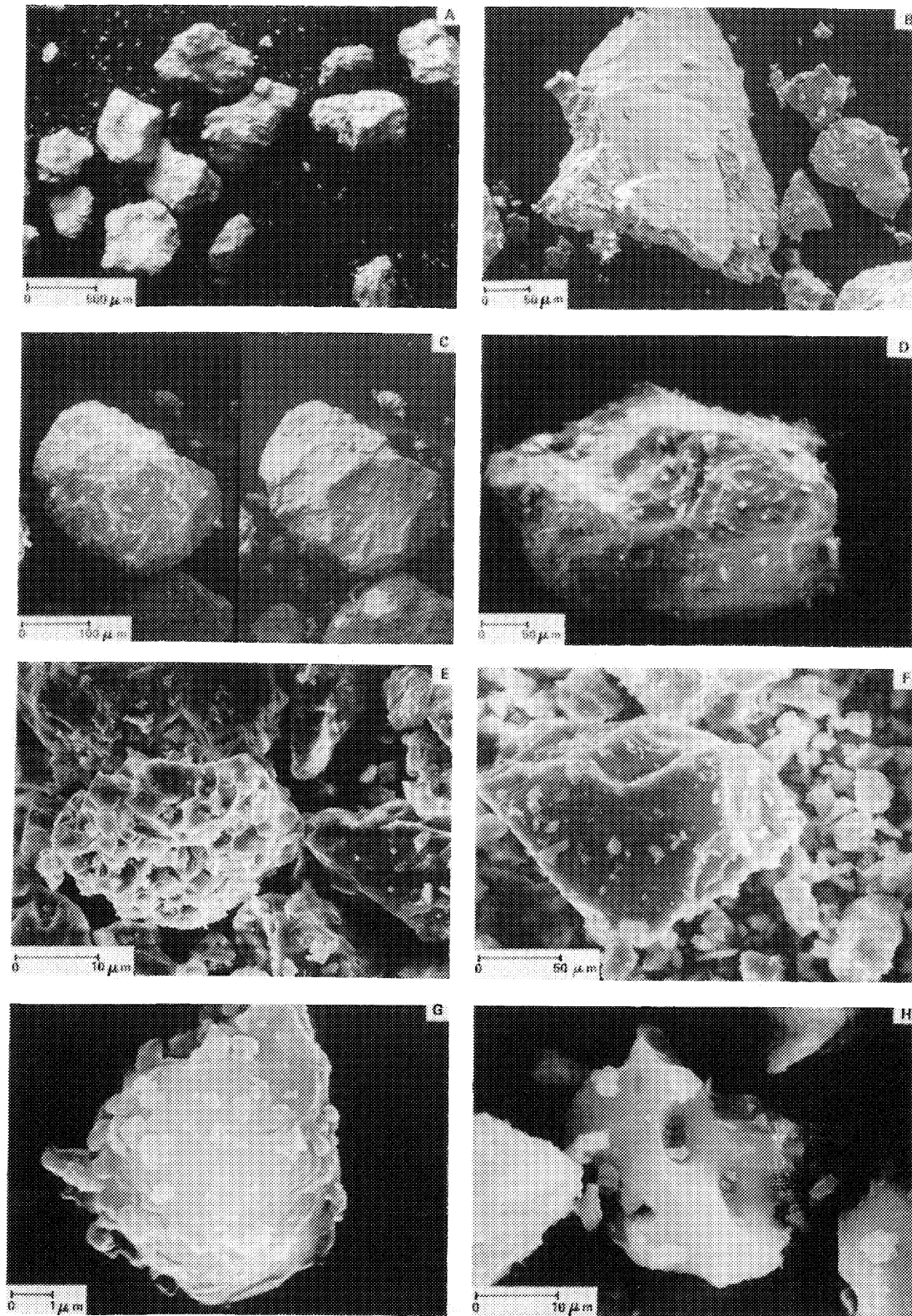
Figure 9. Scanning electron micrographs of tephra erupted from the Mount St. Helens dome. A-D: Coarse particles showing blocky texture, strong surface alteration (C shows both secondary electron and backscattered electron images), and scalloped, rounded edges. E-H: Fine-fraction particles show some vesicularity and abundant adhering dust. Surfaces are mostly fresh in appearance, and grain angularity is high.

TEPHRA TEXTURES
MOUNT ST. HELENS
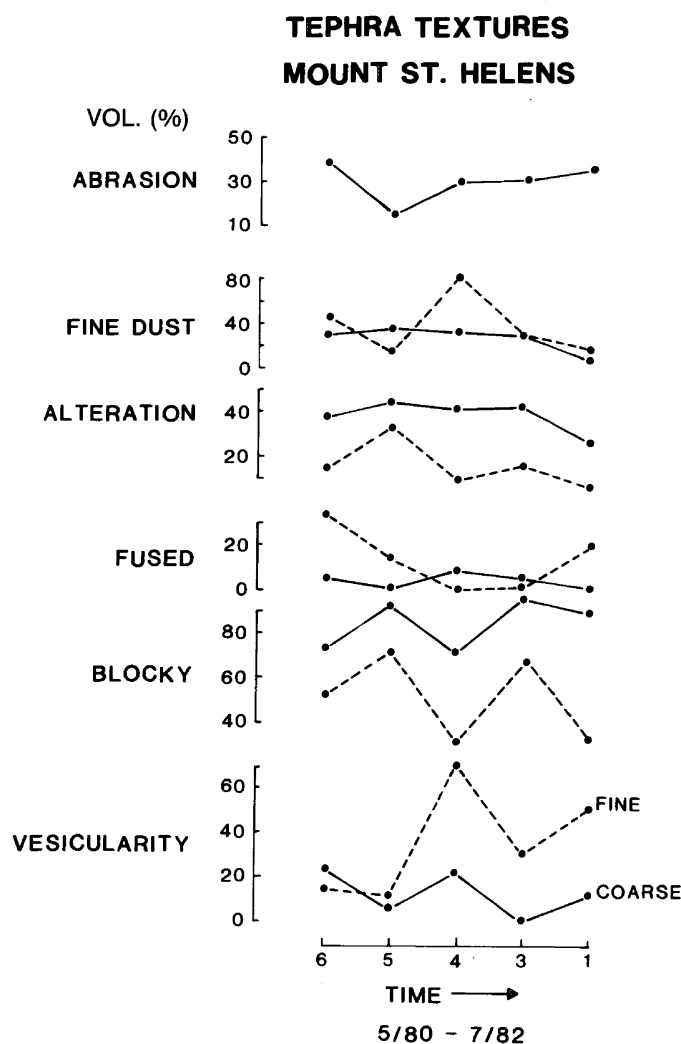
Figure 10. Textural features of tephra from the Mount St. Helens dome. Abundances of the features are obtained from grain counts for coarse and fine (<50 μm) ash fractions and are plotted vs. stratigraphy.

MOUNT ST. HELENS
DOME
TEPHRA SURFACE CHEMISTRY

Figure 11. Major element chemistry of tephra surfaces from Mount St. Helens showing variations of surface alteration with stratigraphy. Average values are shown for all tephra, for the 1980–1982 dome lavas, and pumice from the AD 1500, 1800, and 1980 explosive eruptions (Cashman and Taggart, 1983; Melson, 1983). Note that the tephra analyses are normalized to total 100 wt.% and are standardless, semiquantitative EDS results.

consists of dacite domes and flows; it has been erupting since 1922 (Rose, 1973; Rose, this volume). Sporadic, small eruptions from craters developed over the Caliente and El Brujo vents produce tephra falls and nuée ardentes. The activity can be classified as Vulcanian. Tephra from these eruptions consist of mostly hyalocrystalline, equant, blocky dacite fragments (Fig. 12). Grain surfaces are hackly to conchoidal and have low vesicularities. There are 20% to 30% crystal pyroclasts, including plagioclase and lesser amounts of quartz. Rose (this volume) reports that near the vent there are bread-crust bombs mixed with lithic ash.

PELÉEAN AND MERAPIAN ERUPTIONS:
TEPHRA FORMED BY DOME DESTRUCTION

Explosive disruption or destruction of silicic domes produces tephra composed primarily of poorly vesicular lithic

pyroclasts derived from partly to completely solidified lavas. The main example used here is from the 1902 eruption of Mont Pelée, Martinique. LaCroix (1904) described the eruption as having been laterally directed, whereas Fisher and others (1980) and Fisher and Heiken (1982) interpreted the eruption column as having been vertical, followed by column collapse. In either case, the dome was destroyed and produced a small volume of highly destructive block and ash flows and rapidly moving, high-energy ash clouds. At Merapi, Java, in 1930, part of the dome collapsed and produced pyroclastic flows in which about 10% of the clasts were juvenile (Neumann van Padang, 1931). What all of these eruptions have in common are tephra that consist of mostly lithic pyroclasts formed by fragmentation of dome lavas (Fig. 13).

Mont Pelée, Martinique, 1902 Eruption

The eruptions of May 8 and 20, 1902 were of the most destructive explosive phases of the Mont Pelée eruption. Recent analyses of the pyroclastic deposits indicate that eruptions were
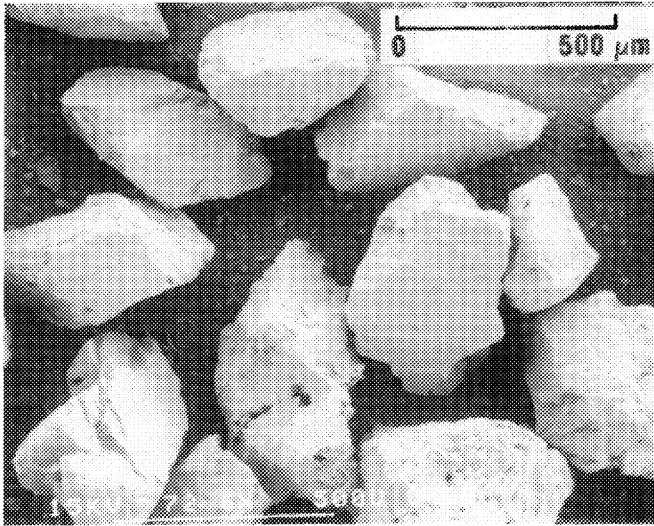
Figure 12. Tephra fall from Santiaguito, Guatemala, 1970 eruption. These are mostly angular lithic clasts that consist of poorly vesicular, hyalocrystalline dacite.

PELÉEAN AND MERAPIAN DOME DESTRUCTION

Figure 13. Schematic illustration of Peléean and Merapian dome destruction, showing initial landslide (A) followed by avalanching and dome explosion (B) caused by explosive release of new, gas-rich magma (center), and explosion of lava flow front (bottom).

vertically directed and that pyroclastic flows were generated by collapse of the eruption column (Fisher and others, 1980; Fisher and Heiken, 1982). There were two parts to these flows; a lithic-rich fraction derived from the dome collapse, which flowed out of a notch in the crater, and a still-fluid portion that may have erupted around the solidified neck and dome. Gravity segregation of coarse lithic fragments concentrated them as block and ash flows in the valley of Rivière Claire and as turbulent, high-energy ash clouds that spread over the landscape.

Tephra from these eruptions are mostly blocky, tabular hyalocrystalline andesite clasts (Fig. 14). Most contain feldspar and pyroxene microlites and some ilmenite and feldspar phenocrysts in a glassy groundmass (80% by volume). Vesicles are rare; vesicularities range from zero to a trace of 1–10 µm-long vesicles, to 10% in clasts having diktytaxitic textures. Coarser blocks and lapilli are similar in appearance and composition. Most of the tephra could have been produced by the breaking up of dome lavas. Glass shards and pumices are present (1% to 50%) and are most abundant in the <63 µm size fraction; they range from simple angular shards to pumices with 60–80% vesicles; most pumices have 4- to 15-µm-long, ovoid, thin-walled vesicles (Fisher and Heiken, 1982). These represent the molten fraction of magma that reached the surface.

Pressure leading to explosive fragmentation of the dome at Pelée could have been caused by magmatic gas, vaporization of ground water, or both. Evidence presented by Fisher and Heiken (1982) is ambiguous as to the phreatomagmatic component of the eruption. Phreatic activity may have triggered the activity, as heavy rains occurred the night before the activity of May 8. Westercamp and Traineu (1983), in their analysis of the past 5000 years of explosive activity at Mont Pelée, noted that a major
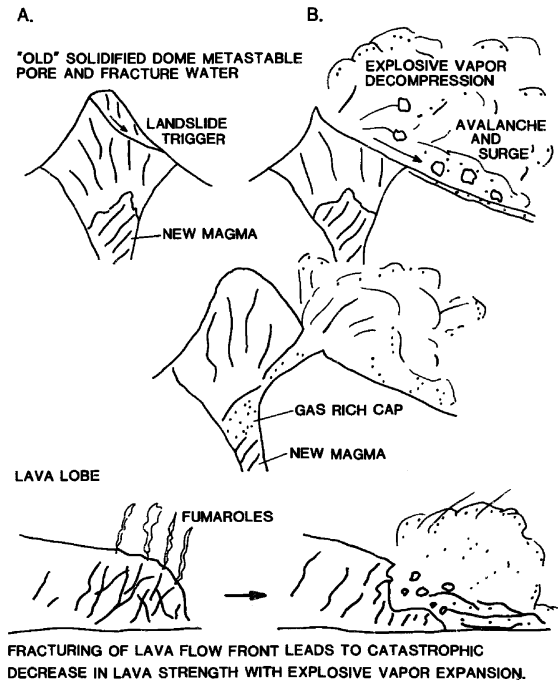
type of eruption (one of four types described) is dome growth and subsequent explosive fragmentation and collapse that feeds glowing avalanches and block and ash flows. This type of activity has occurred during about 60% of eruptions at Mont Pelée.

Differences between Peléean and Merapian activity appear to be little more than timing. Peléean activity occurs during or immediately after dome emplacement, whereas Merapian collapse occurs at some unspecified time after dome emplacement, but while there is still some hot dome lava in the conduit. Tephra deposits and pyroclast characteristics are very similar and may differ only in the amount of juvenile pumice present.

Variations on this tephra type are those associated with explosive disintegration of the foot of a silicic lava flow. Rose and others (1976) have described production of pyroclastic flows following collapse of the nose of a blocky dacite flow (El Brujo flow) at Santiaguito, Guatemala, in 1973. Total volume of erupted material was less than 200,000 m³. Pyroclasts in this deposit are broken crystals, lithic clasts, and vesicular and nonvesicular glass.

PHREATIC TEPHRA

Phreatic eruptions produce accidental lithic tephra during
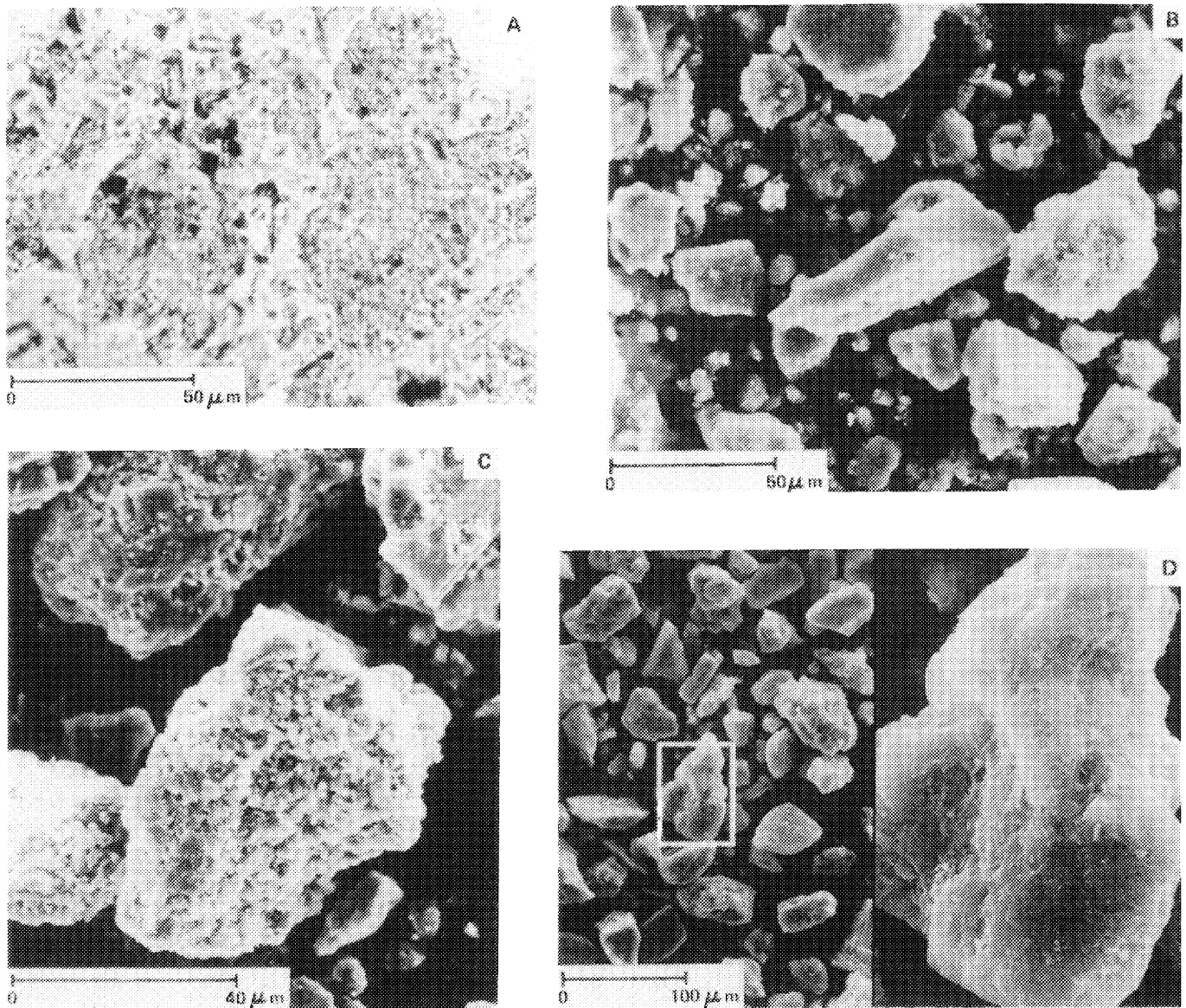
Figure 14. Samples from surge and pyroclastic flow deposits. May 8 and 20, 1902 eruptions, Mont Pelée, Martinique. All samples used here are from the fine-grained matrix of these deposits. A: Photomicrograph (transmitted light) of matrix from block-and-ash flows, unit 1 (Fisher and Heiken, 1982). Over 70% of this sample consists of slightly altered to fresh, angular clasts of hyalocrystalline andesite. B: Scanning electron micrograph (SEM) of matrix from the base of the earliest block and ash flow. Seventy percent of the pyroclasts consist of andesitic lava. Surfaces are irregular and slightly altered. There are also some plagioclase clasts (center). C: SEM of lithic pyroclasts, uppermost block and ash flows. Clast surfaces are very irregular, but angular, with poorly developed diktytaxitic textures. There are traces of pumice in this sample, which is from the uppermost part of the eruption sequence. Smaller pyroclasts cling to grain surfaces, a characteristic of tephra from pyroclastic flows. D: SEM of pyroclasts from the uppermost surge deposits. The deposit consists of 60% hyalocrystalline andesite clasts and 28% phenocrysts (mostly plagioclase). Lithic clasts range from angular to subrounded (inset). There are 1% shards and pumice in this deposit.

PHREATIC DOME ERUPTION
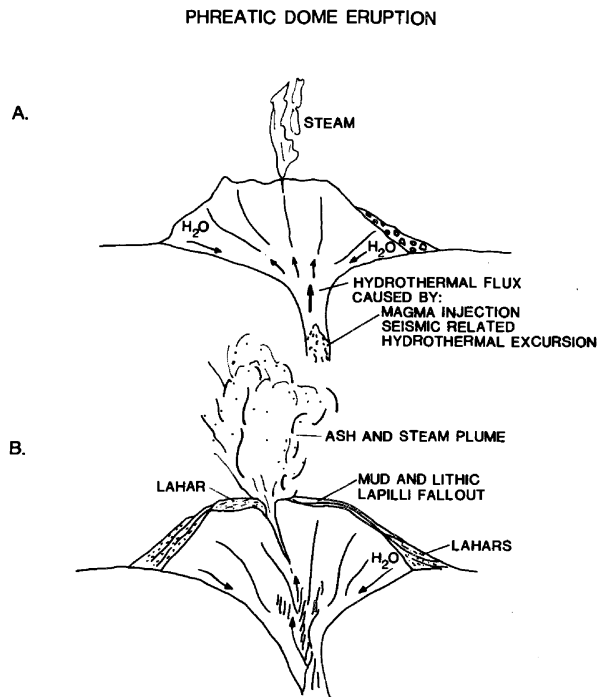
Figure 15. Schematic illustration of phreatic activity where dome is not destroyed. Passive fumarolic stage (A) is followed by energetic steam releases with entrainment of lithic tephra (B).

energetic fumarolic activity and steam explosions associated with hydrothermal processes in domes. This activity may result in slight vent widening and mantling ash and lapilli layers and lahars (Fig. 15), or complete destruction of a dome edifice by steam explosions caused by a new magma pulse beneath the dome.

La Soufrière de Guadeloupe, French West Indies

La Soufrière de Guadeloupe is a steep-sided andesite dome that has had a historic record of explosive phreatic activity. The last such activity occurred during late summer and fall of 1976 and caused evacuation of thousands of residents of the island of Basse-Terre, Guadeloupe. Explosive steam eruptions from open summit fissures and along the southeast flanks of the dome entrained fine-grained tephra that were deposited downwind south and west of the volcano as ash fall and very dilute density currents (Heiken and others, 1980). These tephra formed a gray, thin, sticky deposit that contained accretionary lapilli. During larger eruptions, thin streams of light-gray, steaming mud flowed down dome flanks as lahars (Wohletz and Crowe, 1978).

Tephra from the best-observed phreatic eruption (October 2, 1976), collected about 2 km from the vent, is poorly sorted (σ_ϕ = 2.03) and had a mean grain size of 38 μm (mean grain size [M_z] = 4.7 ϕ). The finer (<38 μm) fraction is composed of lithic and
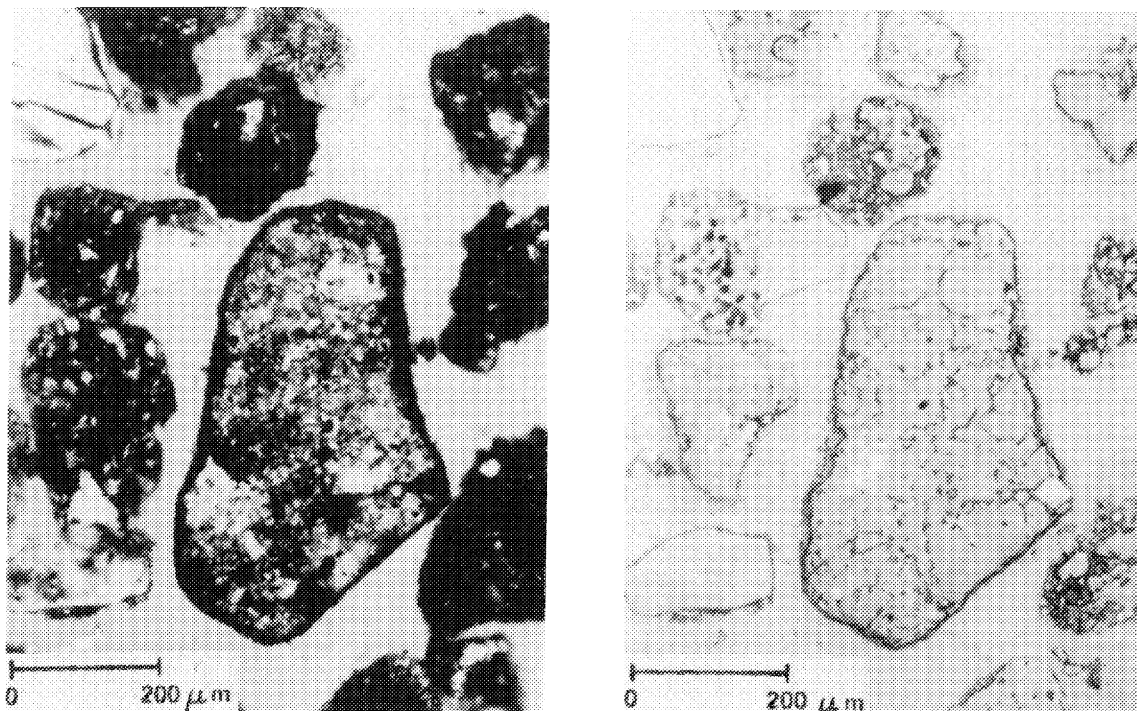
Figure 16. Tephra from the phreatic eruption of September 15, 1976, La Soufrière de Guadeloupe (>38 μm fraction). Left: Transmitted light photomicrograph, partly crossed polarizers. Right: Reflected light photomicrograph. The sample consists of mostly subangular altered lithic pyroclasts; finely crystalline, equigranular lavas derived from dome lavas. Alteration products within lithic clasts include pyrite (bright phases in reflected light), hematite, and clay. Many of the clasts are coated with thin layers of clay.
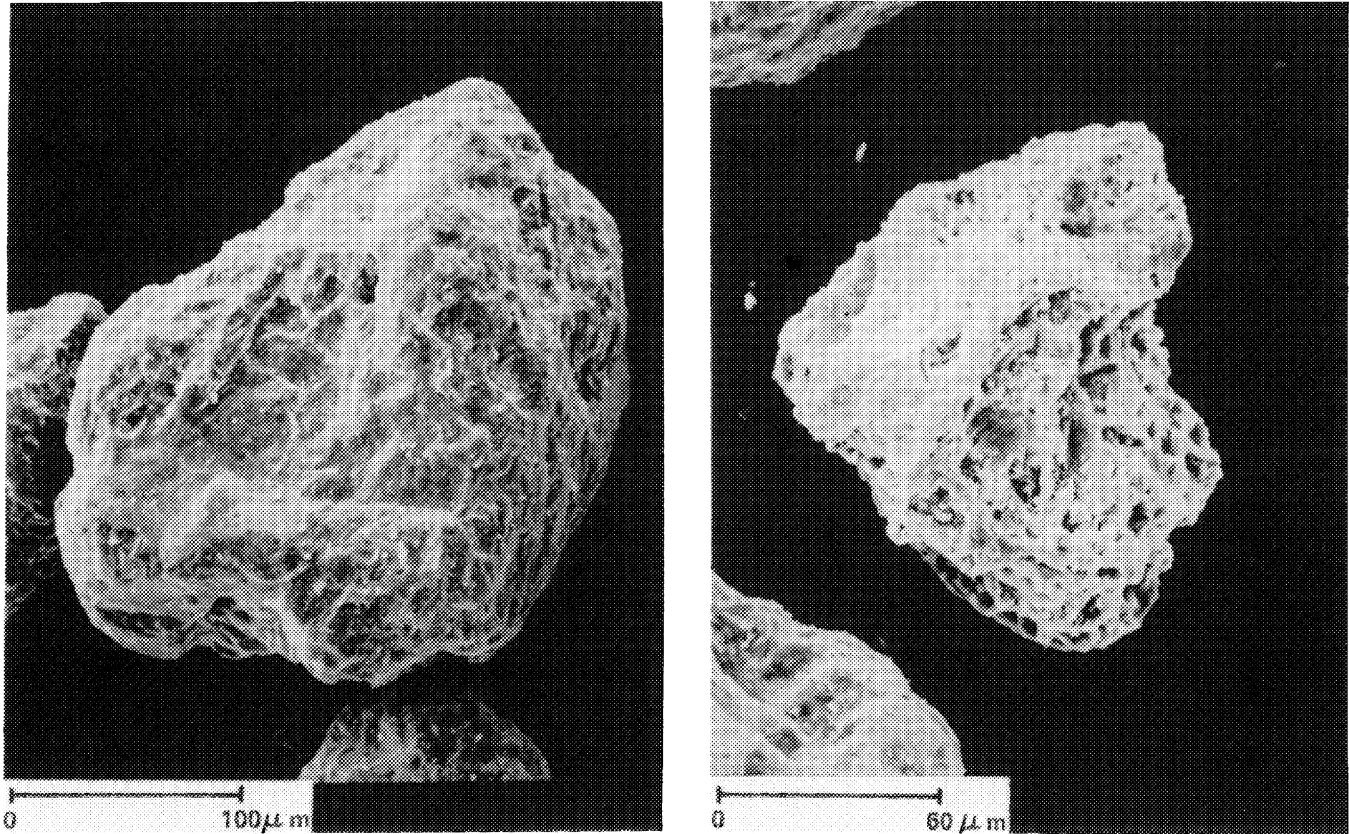
Figure 17. Scanning electron micrographs of lithic clasts from the La Soufrière de Guadeloupe phreatic eruption of August 26, 1976. There are mostly hydrothermally altered, subequant clasts of dacitic lava. All clasts contain pyrite and are partly altered to clay.

mineral fragments, sulfates, sulfides, authigenic silica, and oxides. The coarser fraction was used for modal analysis.

Lithic pyroclasts consist of equant to subequant, subangular to subrounded dacite or andesite fragments that exhibit a wide range of alteration. The most common lithic clasts consist of stubby plagioclase or orthopyroxene phenocrysts in a groundmass of microcrystalline feldspar and pyroxene phases or colorless glass (Figs. 16 and 17). The degree of alteration of these clasts ranges from those that are nearly fresh and have only a trace of hematite stain, through those laced with hematite or pyrite, to those that consist of mixtures of authigenic silica, pyrite, and anhydrite.

Mineral pyroclasts include plagioclase grains that have compositions of An_{50} to An_{88}, and are present as broken, subhedral crystals. As was the case for lithic clasts, mineral phases range from "fresh" (slightly etched grain surfaces) to ragged skeletons. Pyroxene pyroclasts are pale-yellow to pale-pink orthopyroxenes (Wo_3En_{63} Fs_{34}) (Fig. 18). Some of the fresher grains contain 20- to 200-μm-long, brown-glass inclusions. Traces of clinopyroxene are present. Amorphous masses of hematite and 30- to 50-μm pyrite grains are present in small amounts in many

of the samples and as trace amounts in all samples. There are also traces of anhydrite and tridymite.

Most glass pyroclasts are angular, equant, slightly vesicular to nonvesicular fragments that range in composition from andesite to rhyolite (Table 4). Most appear to have been derived from the glassy groundmass of hyalocrystalline dome lavas. Rare colorless glass pyroclasts have 10% to 20% ovoid vesicles (long axes of 10 to 15 μm); nearly all are partly altered and do not represent fresh juvenile pyroclasts. Also present are rare orange-brown basaltic glass fragments that have palagonitic rims.

Tephra from the 1976 phreatic eruptions of La Soufrière de Guadeloupe have been derived from hydrothermally altered and acid-leached dome rocks and older lavas. Lithic pyroclasts and lavas are similar in texture and composition. An abundance of slightly altered to nearly fresh plagioclase grains in the tephra may be related to preferential alteration of the fine-grained or glassy groundmass of the lavas. None of the colorless glass pyroclasts were fresh enough to classify as juvenile tephra. The activity at La Soufrière appears to have been that of a vapor-dominated geothermal system driven by a localized heat source in the form of a magma body located at relatively shallow depths. New magma at

LA SOUFRIÈRE FELDSPARS

+ DOME LAVAS

· TEPHRA

LA SOUFRIÈRE PYROXENES

+ DOME LAVAS
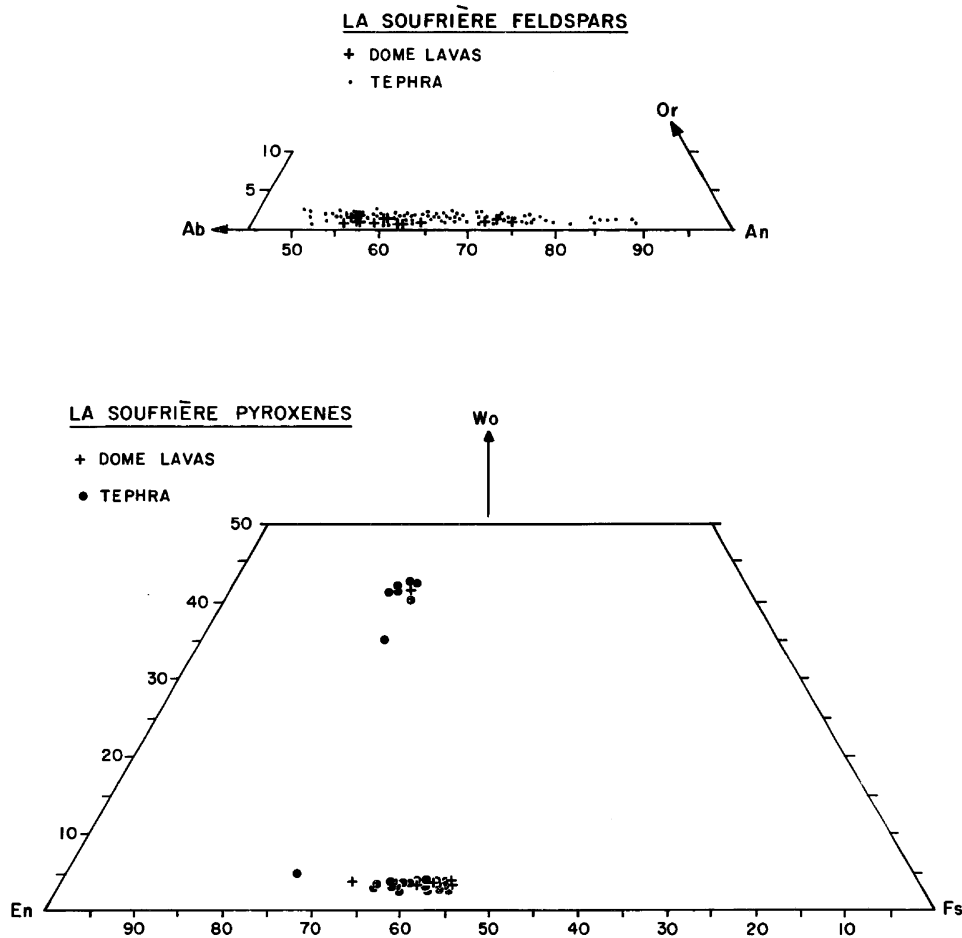
● TEPHRA

Figure 18. Mineral compositions, Soufrière de Guadeloupe. Texturally, the clasts within the phreatic tephra appear to have been derived from the lava dome. Overlapping mineral compositions (pyroxenes and feldspars) also demonstrate this similarity.

depth was suggested by greatly increased seismic activity and shallow epicenters (M. Feuillard, 1977, personal commun.).

Phreatic (violent steam) eruptions without the eruption of magma are common. This type of activity has preceded all magmatic eruptions at Mont Pelée, and often occurs alone (Westercamp and Traineu, 1983). Vapor-dominated hydrothermal systems are often established within silicic domes, where water recharge is at the summit (Healy, 1976). La Soufrière is the highest mountain on Guadeloupe (elevation 1466 m); it consists of fractured, highly permeable lavas, and is the center of high rainfall (Lasserre, 1961). This geologic setting fits models of ground-water movement described by Healy (1976), in which high-temperature fumaroles are present at the summit (1466 m) and warm springs issue from the base (950 to 1200 m elevation) of a volcanic dome. Increased circulation within this system by movement of magma at depth and seismic activity can cause explosive eruptions without magma reaching the surface. Explosive activity was also stimulated after heavy rainfall. Heiken and others (1980) suggested that vapor-dominated fluids eroded vent

fillings and fissure walls within the dome and erupted fine-grained clastic material.

Thin, corridor-like tephra deposits that consist of fine-grained, hydrothermally altered dome rock and are associated with laharic breccias of the same composition may be used to identify periods of explosive hydrothermal activity within domes. Roobol and Smith (1975) have identified such deposits at Mont Pelée, Martinique, where they are interbedded with pumice deposits.

ROLE OF WATER IN FORMATION OF DOME-RELATED TEPHRA

In reviewing studies of explosive eruptions at domes, we have noted in all cases the role of water (liquid and vapor). Although this observation is not unusual in any explosive eruption, we believe that among other physical and chemical variables, the presence and migration of magmatic and meteoric water within the dome before, during, and after an eruptive epoch has

TABLE 4. TEPHRA GRAIN COUNTS OF LA SOUFRIÈRE DE GUADELOUPE
1976 ERUPTION (>38 μm FRACTION)

Component (%)	12 Aug Col Echelle	26 Aug Summit	30 Aug Savanne a Mulet	15 Sept Saint Claude
Plagioclase, unaltered	10.2	15.8	14.9	3.6
Plagioclase, unaltered	4.3	13.3	27.4	2.3
Orthopyroxene, unaltered	4.0	5.3	2.3	3.3
Orthopyroxene, altered	0.9	4.0	---	0.7
Clinopyroxene	0.3	---	0.6	1.3
Pyrite	0.6	2.2	2.9	0.7
Lithic fragments, unaltered	1.9	1.5	1.1	2.0
Lithic fragments, altered	75.8	56.7	45.7	84.4
Colorless glass, altered	0.9	0.3	0.6	---
Brown glass	0.9	0.3	0.6	---
Other	---	---	---	0.6
Total grains counted	322	323	163	307
Sulfur content*	1.7	2.7	4.3	1.3

*Sulfur determined by E. Gladney and D. Curtis, Los Alamos National
Laboratory.

profound effects upon many of the tephra characteristics such as size, shape, and pyroclast surface chemical composition.

Migration of water (aqueous solutions) in dome lavas and its effect upon explosive phenomena and tephra compositions are reviewed in the following section. Migration may occur by a number of different physical processes, including flow along fractures, hydraulic injection from vent walls, molecular diffusion, and mechanical mixing of ground water into rising magma.

Where dome lavas are extruded, decompression and cooling cause diffusion of aqueous species from the lava. The high-temperature fluid that collects in fractures and voids within the lava is also at a high pressure when compared with the atmosphere. The dome rock strength (10 to 100 MPa depending upon composition and fracture density) can balance this overpressure; however, with continued movement and shifting of the dome lava, the mass displays metastable mechanical behavior. Some of the high-pressure steam may vent through fumaroles; this can relieve the overpressure, but can also cause a weakening of the lava by vapor-phase alteration. Continued fracturing, seismic pulses, or renewed heating of the dome by intrusion of a new magma pulse may cause the lava to catastrophically fail, leading to flashing of the confined pore water with subsequent dome explosion. Chemical evidence of this process is shown by vapor-phase mineral deposition in lithophysae and along fracture and foliation planes.

A different type of explosive behavior at domes is a consequence of the extruding dome lava coming into contact with meteoric water in the vent system. Under some circumstances, this contact will cause sudden chilling of the lava, which leads to formation of a network of fractures and lava granulation. In the event that the fragmented lava is more permeable than surrounding country rock, high pore pressures will drive water into the lava along fractures and over grain surfaces. Delaney (1982) has shown evidence of this mechanism along basaltic dike margins.

As a first approximation, these forms of dome water migration can be mathematically expressed as diffusion-type processes where a solute species, water, is moving within silicic, near-solidus magma (models applying Fick's laws of diffusion). We consider two cases of diffusion, the first being that of "slow" molecular transport of one material through another, which has attracted much experimental attention (e.g., Shaw, 1974). The differential equation modeling this case is generally linear and can be solved analytically. In particular, migration of magmatic volatiles from the lava to fracture planes, vesicles, and lithophysae exemplifies this type of diffusion (Fig. 19A). The second case is more difficult to analyze, both mathematically and experimentally, because it involves nonlinear terms in the model differential equation and "fast" mass reaction rates. This case is that of mixing of dome lava with ground water in the vent during extrusion (Fig. 19b). Although the scale of these two cases of diffusion are greatly different, the mathematical treatment discussed below will, we hope, add some insight to field and laboratory studies of domes.

A linear differential equation for the slow case can be writ-

ten (e.g., see, Freer, 1981; Crank, 1975) in one dimension as

$$\partial c/\partial t = D\ (\partial^2 c/\partial x^2) \tag{1}$$

where c, the aqueous species concentration at any time t, and position x, is dependent upon a constant diffusion coefficient D. In order to reach equilibrium, the aqueous species moves through the lava from a concentrated (supersaturated) region to a subsaturated region. Equation 1 is a model of this migration in which water is "accelerated" from its initial localized concentration in the lava toward achievement of uniform distribution. This model requires a mass flux that is linearly proportional to the local concentration gradient. Equation 1, like that of the heat flow equation (Carslaw and Jaeger, 1959), is parabolic and can be solved using the same technique. For a semiinfinite source couple, the solution for c is obtainable using error function (erf) tables for

$$c(x,\ t) = \frac{c_0}{2}\left[1 - erf\left(\frac{x}{2\sqrt{Dt}}\right)\right]. \tag{2}$$

Thus the initial concentration of water in dome lava (c_0) can be used to find how much might accumulate in fractures and pores after a certain amount of time, especially where c_0 is supersaturated at ambient pressures and temperatures. Typically, diffusion constants have been determined from experimental measurements and for this type of system are in the range of 10^{-9} to 10^{-6} cm^2/s (e.g., Freer, 1981).

Because diffusing magmatic water is an aqueous solution of ionic species of Na, K, and other elements, migration of these substances through the lava may be modeled with the Einstein diffusion equation:

$$c = \sigma\ (RT/z^2 F^2 D), \tag{3}$$

where the concentration of the ionic species c, is determined by the electrical conductivity σ, the gas constant R, the temperature T, the ionic charge z, the Faraday constant F, and the diffusion constant for an isotopic "tracer" of the studied species D. This analysis has been found to work quite well for diffusion of Na in obsidian (Carron, 1968). Overall, diffusivity decreases with increasing ionic radius and charge, a result quantitatively shown by Whittaker and Muntus (1970) for basalt. Therefore, where water migration has contributed to explosive behavior at domes, some chemical alteration of the related tephra should be expected, as was discussed earlier for the Mount St. Helens example.

The fast type of diffusion has been less studied, because it behaves mathematically in a highly nonlinear fashion. Situations where effects of grain boundaries, pressure and temperature gradients, and surface tension are present lead to a diffusion coefficient that is spatially dependent upon position. Fick's second law can be expressed as a nonlinear differential:

$$\partial c/\partial t = (\partial D/\partial x)\ (\partial c/\partial x) + D\ (\partial^2 c/\partial x^2). \tag{4}$$

For fast diffusion, D may have values in the range of 10^{-2} to 10^4 cm^2/s, so that the characteristic time scale for this type of diffu-

sion is several orders of magnitude smaller than that of molecular diffusion. In analysis of the origin of these increased values of D, one may examine pressure and temperature effects. Activation energies and volumes have an exponential effect upon D (e.g., Hofmann, 1980); however, Lapham and others (1984) did not find this relationship for rhyolite obsidian at 850°C and pressures up to 500 MPa. In seeking mathematical solutions to equation 4, values of D as a function of c are required from measured $c(x)$ values. Expressing the initial conditions of equation 4 in terms of one variable $\eta = x/t^{1/2}$, c then becomes a function of η only, and equation 4 may be written as an ordinary homogeneous differential equation:

$$-\eta/2\ (dc/d\eta) = d/d\eta\ [D\ (dc/d\eta)], \tag{5}$$

for which the solution may be found by integrating (Shewmon, 1963):

$$-\frac{1}{2}\int_0^{c'}\eta dc = D\ [\ \frac{dc}{d\eta}\ ]\ _0^{c'}, \tag{6}$$

and substituting for η

$$-\frac{1}{2}\int_0^{c'}x dc = Dt\ [\ \frac{dc}{dx}\ ]\ _0^{c'}. \tag{7}$$

In this equation, dx can be considered a function of the fractured lava particle size, which is manifested by tephra grain diameter. With respect to meteoric water migration into silicic magma, initial fragmentation of the magma by thermal stresses provides fractures along which water moves rapidly by thermal hydraulic potential (Delaney, 1982). The effective diffusion is then only a matter of fracture spacing and fragment particle size (the characteristic distance dx, over which diffusion must take place in short times). For tephra with grain diameters on the order of several micrometres, substantial diffusion of various species can occur rapidly so that the bulk composition of fragmented material is altered quickly (e.g., Panum Crater example). This process likely involves solution and redeposition, the effects of which are observable under high resolution microscopy. For example, solution and redeposition may produce rapid changes in $^{18}O/^{16}O$ ratios to a depth of 0.1 μm as was observed in plagioclase in hydrothermal experiments by Giletti and others (1978). At greater depths in the solid material, chemical exchange is much slower.

A more specific treatment of diffusion along fractures and grain surfaces is given by Shewmon (1963), who analyzed grain boundary effects. In this analysis, Fick's second law is expressed with two diffusion coefficients: D_b relating to grain boundary diffusion, and D_l the lattice or "normal" diffusion constant. The effects of these two types of diffusion may be combined into one expression:

$$\frac{\partial c}{\partial t} = D_b\left(\frac{\partial^2 c}{\partial y^2}\right) + \left(\frac{2D_l}{\delta}\right)\left(\frac{\partial c}{\partial x}\right) \tag{8}$$

where x is one half the thickness of the fracture δ, along a grain boundary surface of length y. The solution to equation 8 must

DIFFUSION OF H₂O IN DOME MAGMA

"SLOW"

A EXSOLUTION

⟹ **METASTABLE MECHANICAL BEHAVIOR**

"FAST"

B METEORIC H₂O MIXING

⟹ **TEPHRA COMPOSITIONAL EFFECTS**
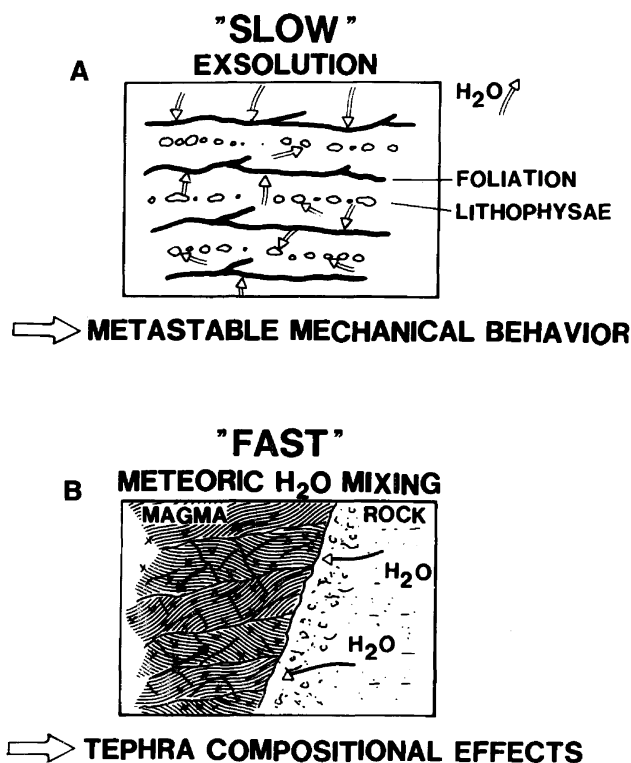
Figure 19. A: Sketch of the diffusion of aqueous species and water in silicic dome lavas. With decreasing pressure and temperature, diffusion concentrates fluids in vesicles, lithophysae, and along fracture and foliation planes. This "slow" diffusion process leads to metastable mechanical behavior of dome lavas. B: Sketch of meteoric waters "diffusing" into silicic magma from saturated country rock. This diffusion can be relatively fast because of surface area and grain-boundary effects caused by fracturing and large thermal gradients.

simultaneously satisfy the "normal" diffusion away from the grain boundary ($\partial c/\partial t = D_1 \nabla^2 c$). An example of this "double" diffusion (equation 8) is shown by Cole and others (1983), who modeled oxygen isotope exchange between fluid and rocks as a two-step process, involving first surface controlled reactions followed by diffusion through the solid material.

Finally, we consider the thermal diffusion effect, which has been named after Soret. It can be mathematically described and applied to systems that have a substantial thermal gradient. Here we subtract it from the flux term of Fick's first law:

$$J = -D \left(\frac{\partial c}{\partial x} \right) - \beta \left(\frac{dT}{dx} \right), \qquad (9)$$

where J is the solute flux, and β is the coefficient of solute flux describing the effect of the temperature gradient, dT/dx. In this situation, a lava dome intruded by new magma can develop a high temperature gradient and some species will respond by migrating either away or toward the higher temperature. Mineraliza-

tion effects found in silicic domes (Burt and Sheridan, 1981) may be one example of this process, which has also been applied to melt differentiation in silicic magma chambers. A temperature gradient in a lava dome prior to renewed eruptive activity can contribute to accidental tephra showing strong chemical alteration.

In the preceding paragraphs we have discussed several diffusion processes that result in an apparent diffusion coefficient that varies greatly from that measured in laboratory experiments. These processes include: (1) "slow" molecular diffusion of aqueous species in near-solidus lava evidenced by lithophysae, vapor-phase crystallization and, in some cases, eventual dome explosion; (2) the effect of local water concentration, which can be analyzed as a function of grain size and is important where dome explosions have resulted from infiltration of ground water into the lava; (3) diffusion enhanced by the effects of grain surfaces in fragmented lava; (4) thermal gradient effects upon diffusion; and (5) the chemical alteration of dome lava by diffusion. In recognition of these various diffusion processes, Cole and others (1983) reported that the overall value of the diffusion coefficient D is fixed by grain size, shape (e.g., sphere, plate), and density, temperature, and water/solid mass ratio (specified rather than concentration c). Future microscopic studies of dome-related tephra may unfold the nature of nonlinear effects on water diffusion in domes.

In conclusion, diffusion of water in dome lavas encompasses a set of related processes that can lead to explosive eruptions. The relationship of diffusion to explosions is simply that it is the process by which volatile species, originally dissolved in the lava, are liberated for explosive expansion with tephra (phreatic and magmatic types). It also generally describes the mechanism of ground water mixing with extruding dome lava, which results in phreatomagmatic explosions. The importance of considering diffusion processes when studying tephra are that they are important underlying processes that contribute to observed tephra size distributions, grain shapes determined with an SEM, surface chemistry, and mechanism of dispersal (e.g., dry and wet surge, ballistic, and fallout).

EXPLOSIVE ERUPTIONS AT SILICIC DOMES AND CHARACTERISTICS OF THE TEPHRA DEPOSITS: SUMMARY

Four general types of explosive volcanic activity accompanying emplacement of silicic domes have been discussed: (1) initial Plinian and phreatomagmatic eruptions preceding dome emplacement; (2) Vulcanian explosions during continuing and episodic dome growth; (3) Peléean and Merapian activity associated with dome destruction; and (4) phreatic explosions preceding magmatic activity or accompanying energetic hydrothermal activity at older domes. Characteristics of the tephra, including volume of the deposit, bedding features, particle size, composition, and textures can be compared and contrasted when assessing explosive activity. These general characteristics are shown in Table 5 and are discussed below.

TABLE 5. DOME TEPHRA CHARACTERISTICS

Eruption Type	Deposits	Size	Tephra Composition	Texture
Initial Vent				
Magmatic	Plinian pumice fall and flow	Coarse (near vent) fall (0 to -3 φ)	Magma composition	Vesicular, angular
Phreatomagmatic	Dry surge	Fine ash (0 to 3 φ)	Slight to moderate surface alteration	Nonvesicular, slablike and abraded
Vulcanian	Wet and dry surge, coarse and fine fallout	Medium to fine ash (1 to 4 φ)	Fresh and altered juvenile, altered lithic clasts	Blocky and equant, nonvesicular to poorly vesicular, rounded
Peleean and Merapian	Poorly bedded avalanche and flow, bedded ash cloud surge	Blocks and ash (-5 to 1 φ)	Fresh magma and lithic clasts	Poorly vesicular and blocky
Phreatic	Poorly bedded, thin ash and lapilli mantles	Fine ash and minor lapilli (-1 to 3 φ)	Altered lithic clasts	Aggregated, complex shapes, "muddy"

Deposits

Bedding features and distribution are perhaps the most distinguishing field characteristic of dome-related pyroclastic deposits. Although deposits of past eruptions may only be partly preserved and exposed in the geologic record, one or more stratigraphic sections can provide ample data to characterize the activity.

Vent-forming eruptions preceding dome emplacement generally produce a sufficient tephra volume (0.05 to 1.0 km³) that deposits near the vent may be up to 10 m or more in thickness; several centimeters of ash may be found over areas of 100 km² or more. Pumice beds and thinly bedded pyroclastic surge layers typify these deposits. The surge beds occur within several kilometers of the vent and are termed "dry" after Wohletz and Sheridan (1983) because they include abundant dune forms, are poorly to non-indurated, have bedding angles of less than 10°, and show little or no soft-sediment deformation features. In flat terrain, surge deposits have abundant dunes near vent and planar bed forms in distal sections (Wohletz and Sheridan, 1979).

Vulcanian eruptions associated with dome growth produce smaller tephra volumes of generally less than 0.1 km³. These tephra form several centimeter- to several meter-thick mantles on the flanks of the volcano. Bedding is characterized by alternating layers (1 to 5 cm thick) of coarse- and fine-grained fallout, dry and wet surge deposits, and lahars near the base of the volcano. Where dry-surge deposits are found on cone flanks, a reversed facies distribution may be found (relative to distribution illustrated by Wohletz and Sheridan, 1979). Planar bedding is common near the vent and dune beds are abundant near the base of the cone. Wet-surge deposits (Wohletz and Sheridan, 1983) are characterized by bedding planes dipping up to 25°, and planar and massive beds, abundant accretionary lapilli, vesiculated tuff, soft-sediment deformation, induration, and strong tephra alteration. Many Vulcanian tephra deposits grade laterally away from the vent into lahars.

Dome and lava-lobe destruction by Peléean and Merapian explosions produce more chaotic tephra deposits, including poorly bedded and sorted pyroclastic flow and avalanche beds that are associated with well-sorted fine layers (ash-cloud surges) (Fisher, 1979; Fisher and Heiken, 1982). These deposits generally thicken downslope and fill drainage areas. Their volume is small (<1.0 km³).

Phreatic tephra layers are typified by their thinness (<1 m and generally less than several centimeters) and extremely small volume (<0.0001 km³). They are also poorly bedded ash and lapilli of muddy appearance and generally very fine grained, except for centimeter- and meter-sized clasts near the vent.

Tephra Characteristics

Particle size distributions, composition, and microscopic grain textures also characterize eruptive style. These features can be qualitatively assessed in the field but lend themselves to detailed quantitative laboratory study.

Peléean and Merapian tephra have the coarsest particles and, in most exposures, include large blocks. Vulcanian and phreatomagmatic tephra are fine to medium ash, and phreatic ash is very fine grained. Plinian tephra is coarse near the vent where exposures are most apparent (see Table 5). Analyses of grain size (such as those presented in Fig. 20) can illustrate information on the relative eruptive energy and dispersal mechanisms that are responsible for preferential sorting and development of size distributions.

Chemical compositions of tephra are rarely reported because of analytical difficulties; however, component analysis reveals important constituents including phenocryst, glass, accessory, and lithic clasts. These data allow interpretation of tephra origin (magma composition and physical properties, hydrothermally altered accessories, and lithic clast types) and emplacement mechanisms that can alter initial constituents. Initial Plinian eruptions distribute tephra that reflect the juvenile magma composition; tephra alteration is minor. Initial phreatomagmatic tephra can be strongly altered; particles have compositions that vary

PUMICE FALL, MEDICINE LAKE   (Heiken, 1978)

PANUM CRATER- PHREATOMAGMATIC   *
       -PUMICE FALL   *
       (SUB-PLINIAN)

VULCANO-SURGE DEPOSITS   (Frazetta et al., 1983)

SANTIAGUITO
    VULCANIAN, 1970   O   (Heiken, 1972)
    FLOW FRONT, 1973   ●   (Rose et al., 1976)

MOUNT ST. HELENS, 1982, DOME TEPHRA   MSH

PELÉE
    AVERAGE, BLOCK AND ASH FLOW   △   (Fisher & Heiken, 1982)
    AVERAGE, SURGE DEPOSITS   ▽

PHREATIC ASH, SOUFRIÈRE DE GUADELOUPE □
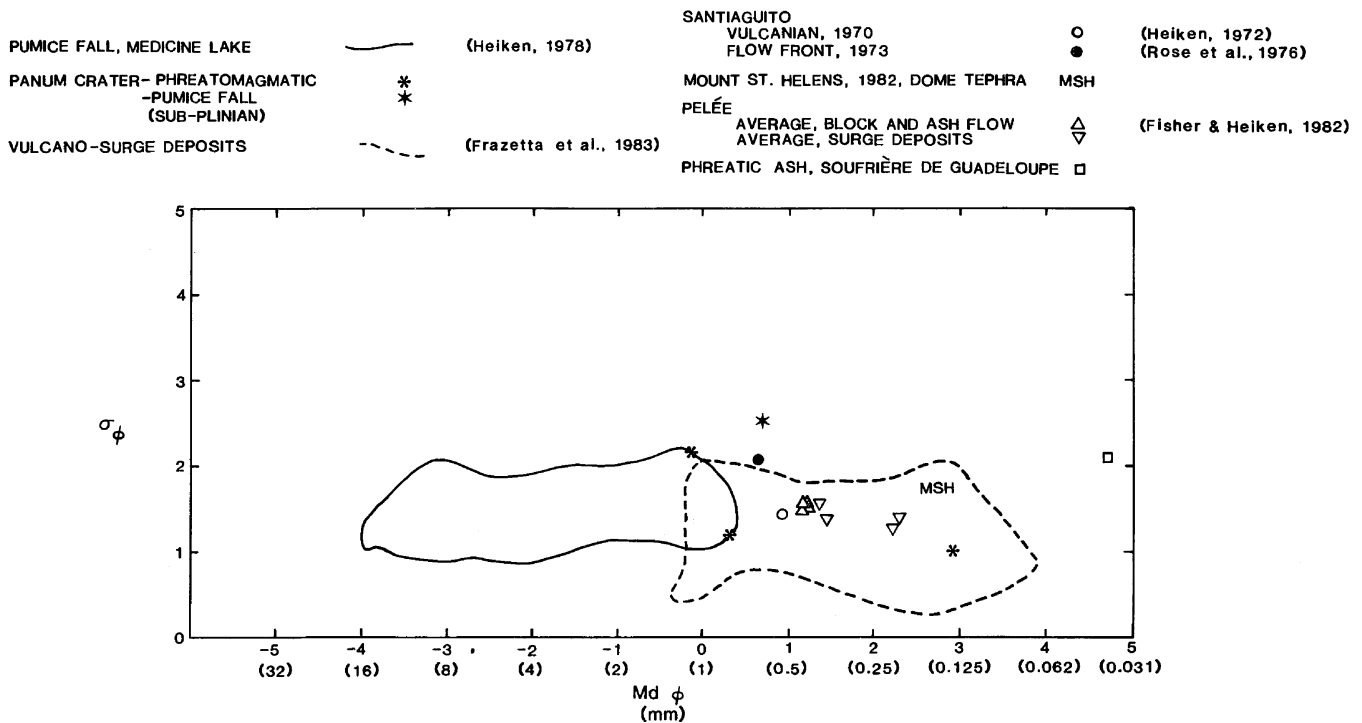
Figure 20. Sorting coefficient (σ_ϕ) vs. median diameter (Md_ϕ) plot summarizing size characteristics of dome-related tephra discussed in this paper.

from fresh juvenile composition to hydrated glass or secondary minerals (see Panum Crater description). Vulcanian tephra have both juvenile magma and lithic components that have altered surface compositions (as described for Mount St. Helens). Peléean and Merapian tephra compositions also display lithic and fresh magma components, but the amount of clast alteration is generally small, except in cases where the dome has been extensively hydrothermally altered. Finally, phreatic ash contains no juvenile clasts and lithic clasts are extensively hydrothermally altered to clays, zeolites, and some sulfides (see section on La Soufrière de Guadeloupe).

Tephra grain textures observed with the SEM have been emphasized in this paper because they show many characteristics, of which only the most general are listed in Table 5. In addition to readily observable textures such as vesicularity and grain shape, the variation among surface features, such as abrasion

scratches, chips, pits, alteration coatings, adhering materials, grain rounding, fracture surfaces, and aggregations provides a complex data set for characterization. This work, still in progress, will require further development of SEM techniques for quantification.

ACKNOWLEDGMENTS

REFERENCES CITED

Burt, D. M., and Sheridan, M. F., 1981, Model for the formation of uranium/lithophile element deposits in fluorine-rich volcanic rocks: American Association of Petroleum Geologists Studies in Geology 13, p. 99–109.

Carron, J-P., 1968, Auto diffusion du sodium et conductivitie électrique dans les obsidiènnes granitiques: Paris Académie de Science, Comptes Rendus, ser. D, v. 266, p. 854–856.

Carslaw, H. S., and Jaeger, J. C., 1959, Conduction of heat in solids, Second Edition: London, Oxford University Press, 510 p.

Cashman, K. V., and Taggart, J. E., 1983, Petrologic monitoring of 1981 and 1982 eruptive products from Mount St. Helens: Science, v. 221, p. 1385–1387.

Crank, J., 1975, The mathematics of diffusion: Oxford, Oxford University Press, 414 p.

Cole, D. R., Ohmoto, H., and Lasaga, A. C., 1983, Isotope exchange in mineral-fluid systems. I. Theoretical evaluation of oxygen isotopic exchange accompanying surface reactions and diffusion: Geochimica et Cosmochimica Acta, v. 47, p. 1681–1693.

Delaney, P. T., 1982, Rapid intrusion of magma into wet rock: Groundwater flow

due to pore-pressure increases: Journal of Geophysical Research, v. 87, p. 7739–7756.

Fink, J., 1983, Structure and emplacement of a rhyolitic obsidian flow: Little Glass Mountain, Medicine Lake Highland, northern California: Geological Society of America Bulletin, v. 94, p. 362–380.

Fisher, R. V., 1979, Models for pyroclastic surges and pyroclastic flows: Journal of Volcanology and Geothermal Research, v. 6, p. 305–318.

Fisher, R. V., and Heiken, G. H., 1982, Mt. Pelée, Martinique: May 8 and 20, 1902, pyroclastic flows and surges: Journal of Volcanology and Geothermal Research, v. 13, p. 339–371.

Fisher, R. V., Smith, A. L., and Roobol, M. J., 1980, Destruction of St. Pierre, Martinique by ash cloud surges, May 8 and 20, 1902: Geology, v. 8, p. 472–476.

Frazzetta, G., Gillot, P. V., LaVolpe, L., and Sheridan, M. F., 1984, Volcanic hazards at Fossa of Vulcano: Data from the last 6,000 years: Bulletin Volcanologique, v. 47, p. 105–124.

Frazzetta, G., La Volpe, L., and Sheridan, M. F., 1983, Evolution of the Fossa cone, Vulcano, in Sheridan, M. F., and Barberi, F., eds., Explosive volcanism: Journal of Volcanology and Geothermal Research, v. 17, p. 329–360.

Fisher, R. V. and Schmincke, H.-U., 1984, Pyroclastic rocks: Berlin, Springer-Verlag, 472 p.

Freer, R., 1981, Diffusion in silicate minerals and glasses: A data digest and guide to the literature: Contributions to Mineralogy and Petrology, v. 76, p. 440–454.

Giletti, B. J., Semet, M. P., and Yund, R. A., 1978, Studies in diffusion—II. Oxygen in feldspars: An ion microprobe determination: Geochimica et Cosmochimica Acta, v. 42, p. 45–57.

Healy, J., 1976, Geothermal fields in zones of recent volcanism: Proceedings of the U.N. Second Conference on Geothermal Energy, Lawrence Berkeley Laboratory, Berkeley, p. 415–422.

Heiken, G. H., 1972, Morphology and Petrography of volcanic ashes, Geological Society of America Bulletin, v. 83, p. 1961–1983.

Heiken, G., 1978, Plinian-type eruptions in the Medicine Lake Highland, California, and the nature of the underlying magma: Journal of Volcanology and Geothermal Research, v. 4, p. 375–402.

Heiken, G., and Eichelberger, J., 1980, Eruptions at Chaos Crags, Lassen Volcanic National Park, California: Journal of Volcanology and Geothermal Research, v. 7, p. 443–481.

Heiken, G., and Wohletz, K., 1985, Volcanic ash: Berkeley, University of California Press, 264 p.

Heiken, G., Crowe, B., McGetchin, T., West, F., Eichelberger, J., Bartram, D., Peterson, R., and Wohletz, K., 1980, Phreatic eruption clouds: The activity of La Soufrière de Guadeloupe, F.W.I., August-October, 1976: Bulletin Volcanologique, v. 43, p. 383–395.

Hofmann, A. W., 1980, Diffusion in natural silicate melts: A critical review, in Hargraves, R. B., ed., Physics of magmatic processes: Princeton, New Jersey, Princeton University Press, p. 387–417.

Hopson, C. A., and Melson, W. G., 1984, Eruption cycles and plug-domes at Mount St. Helens: Geological Society of America Abstracts with Programs, v. 16, p. 544.

Kistler, R. W., 1966, Geologic map of the Mono Craters quadrangle, Mono and Tuolomne counties, California: Geological Survey Quadrangle Map GQ-462, scale 1:62,500.

LaCroix, A., 1904, La Montagne Pelée et ses Éruptions: Paris, Masson et Cie, 662 p.

Lapham, K. E., Holloway, J. R., and Delaney, J. R., 1984, Diffusion of H_2O and D_2O in obsidian at elevated temperatures and pressures: Journal of Non-Crystalline Solids, v. 67, p. 179–191.

Lasserre, G., 1961, La Guadeloupe: Paris, Union Francais d'Impression, 1135 p.

Melson, W. G., 1983, Monitoring the 1980-1982 eruptions of Mount St. Helens: Compositions and abundances of glass: Science, v. 221, p. 1387–1391.

Mercalli, G., and Silvestri, D., 1891, Le eruzioni dell'isola di Vulcano, incomin-

ciate il 3 Agosto 1888 e terminate il 22 Marzo 1890: Relazione Scientifica, 1891, Annuale Ufficiale Centrale Meteorologia e Geodintorno, v. 10, no. 4, p. 1–213.

Neumann van Padang, 1931, Der Ausbruch des Merapi (Mittel Java) im Jahre 1930: Zeitschrift für Vulkanologie, v. 14, p. 135–148.

Newhall, C. G., and Melson, W. G., 1983, Explosive activity associated with the growth of volcanic domes: Journal of Volcanology and Geothermal Research, v. 17, p. 111–131.

Putnam, W. L., 1938, The Mono Craters, California: Geographic Review, v. 28, p. 68–82.

Rittmann, A., 1936, Vulkane und ihre Tätigkeit: Stuttgart, Ferdinand Enke, Stuttgart, 188 p.

Roobol, M., and Smith, A., 1975, A comparison of the recent eruptions of Mt. Pelée, Martinique and Soufriere, St. Vincent: Bulletin Volcanologique, v. 39, p. 214–240.

Rose, W. I., Jr., 1973, Pattern and mechanism of activity at the Santiaguito volcanic dome, Guatemala: Bulletin Volcanologique, v. 37, p. 73–94.

Rose, W. I., Jr., Pearson, T., and Bonis, S., 1976, Nuée ardente eruption from the foot of a dacite lava flow, Santiaguito Volcano, Guatemala: Bulletin Volcanologique, v. 40, p. 23–28.

Shaw, H. R., 1974, Diffusion of H_2O in granitic liquids: Part I. Experimental data; Part II. Mass transfer in magma chambers, in Hofmann, A. W., Giletti, B. J., Yoder, H. S., and Yund, R. A., eds., Geochemical transport and kinetics: Washington, D.C., Carnegie Institution of Washington Publication 634, p. 139–170.

Sheridan, M. F., Moyer, T. C., and Wohletz, K. H., 1981, Preliminary report on the pyroclastic products of Vulcano: Memorandum Sociale Astronomia Italia, v. 52, p. 523–527.

Shewmon, P. G., 1963, Diffusion in solids: New York, McGraw-Hill, 203 p.

Sieh, K., 1983, Most recent eruption of the Mono Craters, eastern central California: EOS (American Geophysical Union Transactions), v. 64, no. 8, p. 889.

Swanson, D. A., Casadevall, T. J., Dzurisin, D., Malone, S. D., Newhall, C. G., and Weaver, C. S., 1983, Predicting eruptions at Mount St. Helens, June 1980 through December 1982: Science, v. 221, p. 1369–1376.

Waitt, R. B., Jr., Pierson, T. C., MacLeod, N. S., Janda, R. J., Voight, B., and Holcomb, R. T., 1983, Eruption-triggered avalanche, flood, and lahar at Mount St. Helens—Effects of winter snowpack: Science, v. 221, p. 1394–1397.

Walker, G., 1971, Grain-size characteristics of pyroclastic deposits: Journal of Geology, v. 79, p. 696–714.

Westercamp, D., and Traineu, H., 1983, The past 5,000 years of volcanic activity at Mt. Pelée, Martinique (F.W.I.): Implications for assessment of volcanic hazards: Journal of Volcanology and Geothermal Research, v. 17, p. 159–185.

Whittaker, E.J.W., and Muntus, R., 1970, Ionic radii for use in geochemistry: Geochimica et Cosmochimica Acta, v. 34, p. 945–956.

Wohletz, K., and Crowe, B., 1978, Development of lahars during the 1976 activity of La Soufrière de Guadeloupe: Geological Society of America Abstracts with Programs, v. 10, p. 154.

Wohletz, K. H., and Sheridan, M. F., 1979, A model of pyroclastic surge, in Chapin, C. E., and Elston, W. E., eds., Ash-flow tuffs: Geological Society of America Special Paper 180, p. 177–194.

——, 1983, Hydrovolcanic explosions II: Evolution of basaltic tuff rings and tuff cones: American Journal of Science, v. 283, p. 385–413.

Wohletz, K., and Krinsley, D., 1982, Scanning electron microscopy of basaltic hydromagmatic ash: Los Alamos National Laboratory document LA-UR 82-1433, 29 p.

Wood, S. H., 1977, Distribution, correlation, and radiocarbon dating of late Holocene tephra, Mono and Inyo Craters, eastern California: Geological Society of America Bulletin, v. 88, p. 89–95.